



## Multi-objective optimization of energy and daylight performance for school envelopes in desert, semi-arid, and mediterranean climates of Iran

Maryam Talaei <sup>a,\*</sup>, Hamed Sangin <sup>b</sup>

<sup>a</sup> Faculty of Architecture and Urban Planning, Ferdowsi University of Mashhad, Mashhad, Iran

<sup>b</sup> Department of Environment, Land and Infrastructure Engineering (DIATI), Politecnico di Torino, Turin, Italy



### ARTICLE INFO

**Keywords:**

Energy efficiency  
Daylight control  
Exterior shading systems  
Passive design strategies  
Multi-objective optimization

### ABSTRACT

Considering global warming as a critical challenge to human life, performance optimization of the building envelope can play a noticeable role to reduce a building's environmental footprint. Meanwhile, shading systems are considered as sustainable passive solutions to contribute to building energy efficiency, and daylight control in early-stage design. Nonetheless, a paucity of research has examined the various shading strategies in diverse climates, particularly arid desert and steppe regions, in conjunction with educational buildings. The present study aims to evaluate the role of fixed exterior shading systems (FESSs), and window-to-wall ratio (WWR) on building' thermal and daylight performance in Iran with desert, semi-arid, and Mediterranean climates. Pareto Frontier and weighted-sum method for multi-objective optimization, and sensitivity analysis were used to study the optimum solutions, and the relationship between the design variables and the performance metrics. Three objective metrics including Spatial Daylight Autonomy (sDA), Annual Sunlight Exposure (ASE), and Energy Use Intensity (EUI), were defined as performance metrics. Shadings include vertical louver, horizontal louver, light shelf, overhang, and egg-crater. The results showed that EUI was reduced via FESS-integrated façade by 25.22%, 20.84%, 19.14%, 14.06%, and 13.47%, in Yazd, Bushehr, Kerman, Rasht, and Mashhad as selected studied cities, respectively. Based on ASE, the horizontal louver surpasses the other systems by 100% ASE value reduction in all climate zones except for Rasht. sDA level is reduced in all climate zones considering five studied FESSs excluding horizontal louver in Yazd and Rasht and overhang in Mashhad by 100% sDA level. Building energy performance simulation is validated by ASHRAE140-2020.

### 1. Introduction

The building sector contributes to energy source depletion, and global warming as two of the most critical human beings' concerns, through consuming more than one-third of global total energy sources and generating about 40% of CO<sub>2</sub> emissions [1]. Meanwhile, building envelopes as an interface connecting indoor and outdoor environments have a noticeable role in building energy efficiency, and paving the route toward sustainable architecture [2,3]. Hence, sustainable building possesses an envelope providing the highest level of indoor environmental quality, and building flexible needs [4]. Façade system and its material also significantly impact on designing carbon- and energy-neutral-building to meet sustainability goals [5–7]. Although the role of an envelope on building energy efficiency was widely studied [8–11], adopting suitable passive design strategies in the early-stage design of buildings in different climates and geographical locations

lacks attention [12]. Besides, considering the challenges of climate change, building envelope optimization to regulate daylight and sun radiation has attracted attention as a fundamental policy for energy-efficient building design [13].

Meanwhile, shadings are among the envelope components with the ability to noticeably control building energy consumption and provide thermal and visual comfort for users [12,14,15]. Adopting an appropriate shade system, which is recognized as a prominent passive design strategy [13], is a vital element to regulate solar heat gain while providing enough daylight for interior spaces, since passive intervention measures aid in mitigating climate change [16]. Mousavi et al. [17] studied the role of passive strategies, including Phase Change Materials (PCM), reflective paint, shading, and natural ventilation, to evaluate their environmental impact. They concluded that these techniques potentially save up to 3000 kgCO<sub>2</sub>eq of Greenhouse gas(GHG). Based on Xue et al. [18] applying passive strategies(thermal insulation, glazing, shading, natural ventilation, and building orientation) resulted in the

\* Corresponding author.

E-mail address: [m.talaei@ferdowsi.um.ac.ir](mailto:m.talaei@ferdowsi.um.ac.ir) (M. Talaei).

Nomenclature	
ASE	Annual Sunlight Exposure
BSh	Hot semi-arid climate
Bsk	Cold semi-arid climate
BWh	Hot desert climate
BWk	Cold desert climate
Csa	Hot-summer Mediterranean climate
DGI	Discomfort Glare Index
DGP	Daylight Glare Probability
E <sub>C</sub>	Energy demand for cooling
ED <sub>tot</sub>	Total energy demand
E <sub>E</sub>	Energy demand for equipment
E <sub>H</sub>	Heating energy
E <sub>L</sub>	Energy demand for lighting
EUI	Energy Use Intensity
EUI <sub>grid</sub>	EUI of grid
EU <sub>lk</sub>	Energy consumption per unit area of typical buildings
Ex	Exterior
Ex-depth	Exterior depth
f <sub>q</sub> (x)	Objective of multi-objective optimization problem
EUI <sub>lk</sub>	Annual energy consumption per unit area
FESS	Fixed exterior shading systems
FA	Floor area
FA <sub>k</sub>	Floor area of building type k
TFA <sub>grid</sub>	The total floor area per grid
GHG	Greenhouse gas
H	Horizontal
H-louver	Horizontal louver
HypE	Hypervolume Estimation Algorithm
i	The iteration result
IES	Illuminating Engineering Society
In	Interior
In-depth	Interior depth
max	Maximum values of optimization sets
min	Minimum values of optimization sets
MOO	Multi-objective optimization
p	Reference points
PCM	Phase Change Materials
PMV	Predicted mean vote
PPD	Percentage of People Dissatisfied
q	Reference points
R	Point Set
S	Point Set
sDA	Spatial Daylight Autonomy
SHGC	Solar Heat Gain Coefficient
st <sub>i</sub>	Occurrence count
SPEA-2	Strength Pareto Evolutionary Algorithm
t <sub>y</sub>	The number of annual timestamps
TDP	Thermal Discomfort time Percentage
UDI	Useful Daylight Illuminance
V	Vertical
V-louver	Vertical louver
w	Weighting coefficient
WWR	Window-to-wall ratio
x	Vector of design variables
X*	Projection of the points

reduction of 13.5–22.4% of life cycle CO<sub>2</sub> emissions.

In addition, researchers looked at the optimization of shading systems and their shape [19–22], as well as other envelope factors such as window-to-wall ratio (WWR) [21,23], orientation [24], geometry [25, 26], and glazing material and type [11,21,27], on thermal, visual and energy performance [15,28] of the building as key passive design strategies integrated with early-design stage. However, limited research has compared different shading systems in different climate zones to optimize building visual, thermal, and energy performances. Table 1 shows key literature on building envelope optimization.

In the educational buildings, controlling lighting quality with an appropriate shading system is of great importance in terms of its considerable effect on students'/teachers' productivity and healthiness, as well as building energy conservation [39]. Subhashini and Thirumaran [40] studied the role of vertical fines and horizontal overhangs applied in an educational building to enhance the thermal performance of the classroom. They concluded that, for total shade (100%) vertical fines with 0.6m depth perform better than overhangs longer than 1 m in terms of both technical and financial factors. Through adopting passive design strategies, including static shading devices, Zhang et al. [11] showed a reduction in energy use for heating and lighting by 24–28% while the increase in thermal discomfort and Useful Daylight Illuminance (UDI<sub>100-2000lux</sub>) by 9–23% and 15–63%, respectively. Using PCMs as a passive shading strategy for retrofitting an educational building, Park et al. [41] could show the reduction of cooling energy demand by 44% and increasing thermal comfort hours by 34%.

Nonetheless, there are currently few studies comparing various shading systems to increase energy efficiency, thermal and visual comfort in classrooms situated in various climates, despite the many benefits of using passive measures in educational building design. Despite different research on educational buildings and their environmental performances, studies still expound on critical deficiencies in classroom design, such as low levels of air quality and energy efficiency [42,43], as

well as thermal comfort deficiency [44].

In Iran, with double energy consumption in the building sector compared to the average global energy use [45], taking energy-efficient strategies for building design is regarded as a critical measurement to address global warming [45,46]. Moreover, educational buildings in Iran are among the most energy-consuming sectors in the nation, with their energy consumption 2.5 times higher than that of developed countries [27]. In this sense, some researchers focused on the thermal and visual comfort performance of educational buildings in Iran via adopting passive strategies. However, very limited research examined the role of passive strategies especially shading systems, on the environmental performance of schools. Ziae and Vakilnezhad [47] improved daylight and thermal comfort in a classroom by investigating optimal characteristics of light shelves and WWR proportion in Tehran with a Cold semi-arid climate(Bsk) and Sari with a Hot-summer Mediterranean climate(Csa). They concluded that considering the optimum option for mentioned building performance objectives, WWR has greater value in Tehran than Sari. Khani et al. [27] also optimized the energy, thermal, and visual performance of school classrooms via passive design variables such as window characteristics and shading devices etc.

The Organization for Development, Renovation and Equipping Schools (DRES), established in 1975, related to the Ministry of Education and Plan and Budget Organization of Iran, is responsible for specifying national codes and standards (e.g., Code 697) for designing, renovating, and constructing the school. Although one of the essential responsibilities of these codes and guidelines was determined to design climate-based schools, no particular regulation and guidelines were specified to address the daylight performance of such buildings [47] as passive strategies like different shading devices, especially under various climatic conditions in Iran. Meanwhile, only some general recommendations for thermal/visual comfort were presented in Ref. [48] Published for DRES.

**Table 1**

Literature on multi-objective optimization of the building performance with an emphasis on shading systems.

Ref	Location	Building type	Objective	Variable	Type of Shading	Simulation & Optimization method Tool
[8]	Xiong'an, Beijing	Gymnasium	Daylight illuminance, Daylight Glare Probability (DGP), solar radiation	Facade shading ratio	Vertical metal Louvre	Honeybee + Ladybug, Octopus (SPEA-II)
[19]	Kitakyushu, Japan	Office	ASE, SDA, UDI, View	Shading	Expanded-metal shading (Bond, length, height, strand, angle)	Honeybee + Ladybug, Octopus (HypE)
[27]	Qeshm Island, Iran	School	Total energy consumption, predicted mean vote (PMV), percentage of people dissatisfied (PPD), UDI <sub>100-2000 lx</sub> , sDA	Building orientation, number/depth/angle of shades, glazing material, WWR, shading distance	Horizontal shading device	Honeybee + Ladybug, Genetic algorithm
[29]	Tehran, Iran	Office	Electricity Consumption, Discomfort Glare Index (DGI), PMV	Shading system characteristics	Venetian blinds	JEPLUS + EA NSGA-II
[30]	Hohhot, Tianjin, Shanghai, Guangzhou, China	Office	Cooling/heating/lighting/energy consumption, Discomfort hours	Building orientation, window inside/outside/medium layer material, overhangs angle/depth	Overhang	JEPLUS + EA NSGA-II DesignBuilder
[28]	Nanjing, China	Office	UDI <sub>100-2000 lx</sub> , EUI, and Thermal Discomfort time Percentage (TDP)	Openable-window-area ratio, WWR, solar-heat-gain-coefficient (SHGC), louver depth, wall thickness	Louver	Honeybee, EnergyPlus, Radiance + Ladybug, Octopus
[11]	Tianjin, China	School	Energy demand, summer discomfort time, UDI <sub>100-2000 lx</sub> .	Orientation, depth of classroom/corridor, glazing ratio of the interface, glazing material, shading type	Venetian blinds and roller shading	Ladybug tools, Radiance, EnergyPlus, Octopus.
[31]	Amol, Iran	Residential	EUI, UDI <sub>100-2000 lx</sub> , PPD	Building wall/roof, roof/wall insulation, WWR, skylight, veranda, shading, glass type	Veranda shading device	Ladybug tools, Radiance, OpenStudio, EnergyPlus, Octopus.
[25]	Miami, Atlanta, Chicago	Office	EUI total (Heating, Cooling, lighting), UDI <sub>100-2000 lx</sub>	Building depth, roof ridge location, skylight width/length/location/orientation, south/north window width, louver length	Louver	Ladybug tools, EnergyPlus, Radiance, Octopus.
[32]	Madrid, Spain	Residential	Summer/annual overheating, Energy demand (heating, lighting), Thermal/lighting discomfort.	Shading shape area	Static external kit-based shading devices	EnergyPlus, Harmony Search Algorithms + Pareto Front approach
[33]	Houston, USA	Office	Cooling load, sDA <sub>300/50%</sub>	Hourly behavior of openness scenario	Climate adaptive building envelope (CABE)	Ladybug, Honeybee, EnergyPlus, Octopus, MOO + parametric behavior map (PBM)
[9]	Niš, Serbia	Residential	Energy required heating/cooling number of discomfort hour	WWR sunspace, orientation, sunspace/façade glazing type, shading type, Façade wall structure	Brise-soleils, Horizontal/vertical awning	EnergyPlus, DesignBuilder, NSGA-II
[34]	Rome, Italy	Residential	Total energy demand (ED <sub>tot</sub> ), Investment cost, CO <sub>2</sub> emissions, Annual energy cost	Building shape/geometry/orientation, WWR façade materials, Glazing type, Shading, Courtyard greenhouse, sunspace, passive/active strategies	Brise-soleil	Genetic algorithm, EnergyPlus
[35]	Bangkok, Hong Kong, Guangzhou, Taipei	Residential	Cooling/lighting energy demand	Building orientation, WWR, shading, natural/mechanical ventilation	External obstruction overhang	EnergyPlus, NSGA-II, Weighted-sum method
[10]	Hong Kong, Los Angles	Residential	Cooling/heating/lighting energy demand	Building layout/geometry/infiltration & air-tightness, envelope thermophysics.	External obstruction, overhang	EnergyPlus + JE + R multiple linear regression (MLR), multivariate adaptive regression splines (MARS) and support vector machines (SVM), NSGA-II,
[36]	Mashhad, Iran	Residential	Energy consumption (heating/cooling/electrical), PPD	Light shelf design parameters (angle/depth/number)	Light shelves	Ladybug, Honeybee, EnergyPlus, OpenStudio Radiance, Daysim
[37]	Bandung, Indonesia	office	sDA, ASE, DGP	Type of blinds (Horizontal/vertical), slat angle, blinds material specularity	Horizontal/vertical blind	Grasshopper + DIVA Ladybug + Honeybee Graphical optimization method using Pareto frontiers
[38]	Nanjing, China	Educational (School)	Annual energy consumption (Artificial lighting, Heating, Cooling, Fresh air), thermal comfort, cost	Solar absorptivity/Thickness/Thermal conductivity of external wall, WWR, fine (depth/angle), overhang (depth, angle/height)	Overhang, fin	Artificial neural network (ANN) model + multi-objective particle swarm optimization MOPSO + NSGA-II EnergyPlus + Python

In the other very recently published draft documents by DRES, School Green Management Reference Guide(Code 847), designing school shading was referred to the National Building Codes of Iran (Code19) published by Road, Housing and Urban Development Research Centre, which only specifies vertical and horizontal fines for different climate zones of Iran merely based on their angles. It is also a general guide which was not defined based on any specific building function like an educational building. Furthermore, there is a lack of research comparing the effectiveness of various external/interior shading systems via optimization to manage daylight performance of the buildings, particularly educational ones, as well as their thermal, visual, and energy assessment for various climates. To maximize building thermal and energy performances, the majority of research took into account certain and limited kinds of shading or climatic zones (Table 1). The present study aims to improve the daylight and energy performance of school buildings by studying the optimized characteristics of fixed exterior shading systems (FESSs) related to WWR in five different climate zones of Iran, including all arid climate types(B) and Mediterranean climate based on Köppen climate classification and define the best solutions. It also evaluates and compares the performance of exterior shading devices under the mentioned climate conditions, where all have hot/warm summers, and shadings are critical passive strategies for controlling sun radiation and cooling energy demand [49].

Shading systems provide a healthy environment by preventing buildings from overheating by controlling solar radiation, cooling energy demand reduction, and bestowing users with reduced glare levels, thermal comfort, and private circumstances [50]. Dakheel and Tabet Aoul [51] classified shading systems as active and passive. Passive shadings refer to typical interior/exterior fixed shading devices, while active ones adapt to their circumstances and users' needs by changing their features [52]. Recently, active systems and shading like bio-adaptable shading [53], smart [54,55], energy-generating glazing [56], and shading [57] have drawn attention in terms of their potentiality to actively adapt to changing climate conditions [51,58] and their superiority to static shadings in terms of cooling energy saving [59]. Nonetheless, because of their affordability and ease of use, static shading devices continue to be more often used as passive solar radiation management strategies than adaptive ones [60,61]. Accordingly, prior research has addressed several facets of the drawbacks and difficulties associated with adaptable facades [62].

Tsangrassoulis [63] classified shading devices based on their angular selection, positions considering window glazing, and movability. Bellia et al. [64] categorized shading systems as fixed and moveable (manual/automatic) in internal/extremal or intermediate glazing position, as well. They enumerated main shading types as overhangs, horizontal louver(H-louver), vertical louver(V-louver), blinds, light shelves, and a combination of overhang and side fines. Kirimtak et al. [49] introduced fixed shading devices, such as overhang, V-louvers, H-louver, and egg-crates, while specifying moveable ones such as Venetian blinds, vertical blinds, roller shades, and deciduous plants.

Furthermore, different research evaluated the performance of shading devices on daylight and energy performances of a building. Atzeri et al. [65] compared interior/exterior shading systems to evaluate the thermal, visual, and energy performance of an open space office in Rome, Italy. The findings show that whereas interior shading causes a rise in the cooling load, external shading reduces cooling and increases heating energy consumption. The optimal features of an interior fixed/adaptive shading system were studied by Mangkuto et al. [61] in order to improve the daylight performance of a high-rise office building in Bandung, Indonesia, which has a tropical environment. Results showed that adaptive shadings can provide  $sDA_{300/50\%} \geq 74\%$  and  $ASE_{1000,250} \leq 12\%$  for all zones. De Luca et al. [59] compared the role of static and dynamic shading devices on energy use of an office building in Tallinn, Estonia, and concluded that moveable shading outperforms static ones due to providing uniform performance. De Luca et al. [66] demonstrated energy efficiency in a FESS-integrated office building in

Milan, Tallinn, and Cairo by 25%, 28%, and 45%, respectively. Elouadjeri et al. [67] assessed the effect of the configuration of FESS on thermal, daylight, and energy consumption of buildings in Ghardaïa, Algeria, with a hot, dry climate. The results indicated that all design options decreased  $sDA_{500}$ , although it was still above accepted value (55%). Besides, 19% energy savings were achieved by reducing the cooling load, thanks to the light control potential of FESS. Nevertheless, heating and annual energy demand augmented by 38% and 22%, correspondingly.

In general, external shadings perform more effectively than internal shadings to reduce cooling energy demand, especially in hot climates [49]. When it comes to preventing glare, interior light shelf components beat external elements in this regard [63]. As a result, several studies have examined how exterior shading affects energy [68,69], thermal performance [70], how energy, daylight and thermal comfort work together [67], or how energy-saving and visual comfort [71] relate to sustainability performance as a subset of performative computational architecture [72]. Despite extensive literature on various types of shading devices like light shelf [47], louvers [28], blinds [29], and overhangs [68], optimizing properties, and the comparison of different FESSs applied on school building envelopes in different climates to improve daylight and visual performance of the building was not studied by previous research, extensively. The present study focused on the role of FESS (V-louver, H-louver, light shelves, overhang, and egg-carte) [49, 73] concerning WWR to enhance building energy efficiency and daylight performances of school buildings and compare them in different hot/warm summer climates of Iran. Furthermore, the light shelf falls under the least researched categories for improving the building's sustainability performance [72]. While there has been some study on light shelves [36,47], there are currently few studies that compare the performance of this device to other systems using a multi-objective optimization (MOO) technique. Moreover, to the author's best knowledge, no previous study studied the role of exterior shading devices in school buildings in the desert and semi-arid Köppen climate (B) classification in the world. Accordingly, the novelty of this paper is based on bridging the research gap in the field of passive design strategies and Performative Computational Architecture by proposing an MOO framework to develop a high-performance school building designed with different shading devices. On the other hand, there is no codes, or standard to address high-performance school design regarding different shading systems to enhance sustainability performances of such buildings, in Iran. Therefore, the goal of the research is to enhance the energy and daylight efficiency of educational buildings by examining the optimal features of FESS in relation to WWR in five distinct Iranian climates (which together account for more than 98% of the nation's land area)

## 2. Material and method

This study follows three steps to develop the research framework presented in Fig. 1.

**Step 1** determined the simulation model by generating a base parametric model, and identifying design variables for simulation and MOO. Thus, in this step, energy and daylight performance simulations were run for the base case with a south-orientated window (Section 2.3) located in different defined climate conditions (Section 2.2).

**Step 2** applied the MOO approach for five shading design scenarios in the school building in five Köppen climate classifications to improve the sustainability-oriented performance by reducing energy use intensity (EUI), and improving daylight by making a balance between Spatial Daylight Autonomy(sDA), and Annual Sun Exposure (ASE). Climates include Hot desert (BWh), Cold desert (BWk), Hot semi-arid (BSh), Cold semi-arid(BSk), and Hot-summer Mediterranean(CSa) Climates. The independent variable for optimization

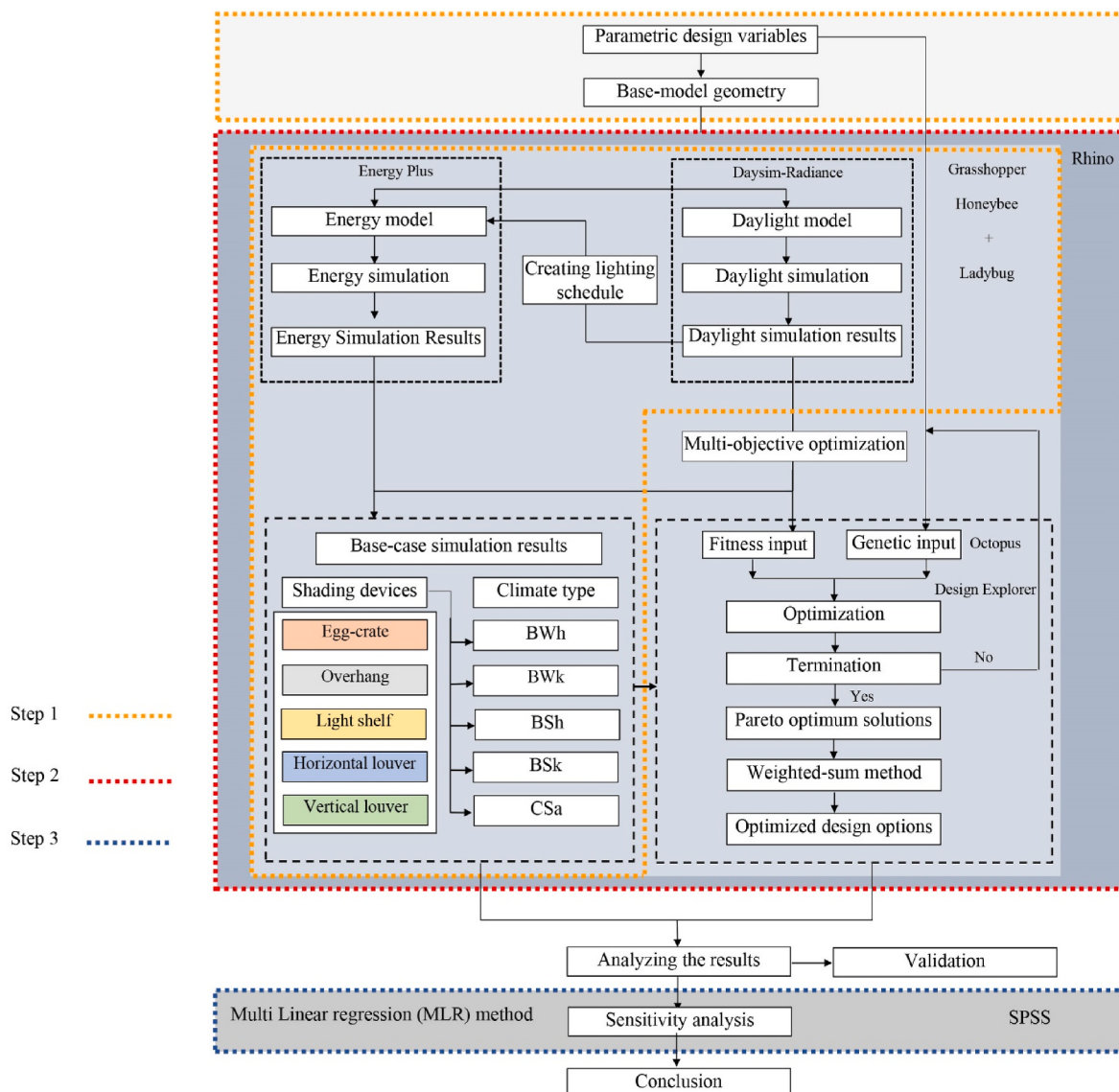


Fig. 1. Research framework.

includes shading properties (angle and dimension), and WWR. In the next stage of MOO, the weighted-sum method was applied to define, and discuss absolute Pareto optimum solutions.

**Step 3** used sensitivity analysis considering the optimum design options to study the sensitivity of performance metrics.

Finally, for the first time, this study evaluated and examined the result accuracy of the simulation software Ladybug Tools (LBT version 1.6.0) released in 2023-January-17 based on ASHRAE Standard 140–2020 via comparison method.

## 2.1. Simulation

In the present study, the energy simulation is to define annual energy loads (cooling, heating, lighting, and equipment) as EUI ( $\text{kWh}/\text{m}^2/\text{yr}$ ), including mentioned energy types used within the building divided by gross floor area [25,74,75]. Besides, other research explored associated ideas such as EUI of grid( $EUI_{grid}$ ), which is calculated based on spatial information and energy consumption per unit area of typical buildings ( $EUI_k$ ) [76]. To calculate EUI and EU and total floor area(FA) based on each grid, formulas (1) and (2) are applied:

$$EU_{grid} = \sum_{k=1}^n EUI_k \times FA_k \quad (1)$$

$$EUI_{grid} = \frac{EU_{grid}}{TFA_{grid}} \quad (2)$$

Where  $EU_{grid}$  and  $EUI_{grid}$  are annual building energy consumption per grid, and annual energy consumption per unit area of a grid, respectively.  $EUI_k$  is the annual energy consumption per unit area, and  $FA_k$  is the floor area of building type  $k$ .  $TFA_{grid}$  is the total floor area per grid.

The other studied performance metrics are sDA and ASE, defined by the Illuminating Engineering Society (IES) [77] as an evaluation indicators for building daylight performance. Considering temporal and spatial dynamics of daylight in buildings [78], the sDA metric defines the adequacy of daylight level on the work plan during annual hours worked. IES characterizes  $sDA_{300/50\%}$  as the minimum illumination of 300lx for 50% of occupied hours(8 a.m. to 6 p.m.) during a year. Taking the N-point grid and determining  $ST(i)$  with value as one for every grid point receiving minimum needed illuminance for more than a given fraction of total occupancy time, sDA is calculated by the formula(3):

$$sDA = \frac{\sum_{i=1}^N ST(i)}{N} \text{ with } ST(i) = \begin{cases} 1 : st_i \geq \tau t_y \\ 0 : st_i \leq \tau t_y \end{cases} \quad (3)$$

Where  $t_y$  is the number of yearly timestamps showing the temporal fraction threshold and  $st_i$  is the occurrence count that the sDA illuminance threshold at point  $i$  is exceeded [79]. According to this research, the classroom's necessary sDA minimum daylight level is 500 Lux [80]. Evaluating undesirable direct sun radiation, ASE index is defined as the percentages of floor area accepting minimum defined illuminance for at least the specified occupied hours through a year. Furthermore, as IES defines, ASE<sub>1000,250h</sub> indicates space percentage receiving above 1000lx during more than 250 occupied hours. Identical to sDA, ASE index is assessed by formula (4):

$$ASE = \frac{\sum_{i=1}^N AT(i)}{N} \text{ with } AT(i) = \begin{cases} 1 : at_i \geq T_i \\ 0 : at_i \leq T_i \end{cases} \quad (4)$$

LEED ver.4 requirements define sDA<sub>300/50</sub> for at least 55–75% and ASE<sub>1000,250h</sub> for less than 10% of the occupied floor area. In this research, daylight and energy simulations were fully integrated to provide energy saving for buildings considering cooling, heating, lighting, and equipment energy consumption caused by daylighting, and controlled by shading systems [25]. The light control system has been used in the simulation model to adaptively switch on/off or dim depending on the stated illuminance threshold in order to accomplish this goal. Hence, a lighting schedule for the entire year was created to be imported into the energy model to integrate energy consumption of lighting, cooling, heating, and equipment considering daylighting level. The schedule was determined between 8am and 6pm during a typical year. Therefore, the spatial grid size for daylighting sensors placement to calculate sDA and ASE was assumed to be about 0.5 × 0.5 m, 0.7 m above the floor in the parametric model.

To conduct the simulation and optimization process, 3D Software McNeel Rhinoceros and Grasshopper, known as a parametric modeling program [81], were applied to create the base geometry model. Then, Honeybee and Ladybug [25,82], as environmental plugins for Grasshopper to run light and energy simulations, were included in the simulation process. Literature reviewers (Table 1) have shown an interest in Grasshopper for Rhin3D, as well as the Honeybee and Ladybug plugins, which are among the most used programs for solving MOO problems. In addition, OpenStudio [83] and the EnergyPlus engine [84] were used to do building energy simulations. Result validation is also defined using case No.600(BESTest) in the ASHRAE Standard 140–2020 [85] to evaluate building energy analysis.

For daylight simulation, the software Daysim based on the widely applied and validated simulation engine Radiance [86], was employed. Daysim using the daylight coefficient approach integrated with the Perez all-weather sky model [87], was developed to contribute to assessing illuminance/luminance time series considering diverse sky conditions and was validated by different research [87,88] through CIE test cases [89]. Radiance parameters are presented in Table 2.

## 2.2. Locations and climates

The present study is to investigate the role of FESSs on the energy and

**Table 2**  
Radiance parameters used in the study.

Parameters	Description	Value
-ab	Ambient bounces	6
-ad	Ambient divisions	1024
-as	Ambient super-samples	512
-ar	Ambient resolution	256
-aa	Ambient accuracy	0.1

daylight performance of school buildings in almost all climate zones of Iran. Hence, different climate classifications were investigated, comprehensively. Iran's climates are classified by Ganji [90], Dehsara [91], Djamali [92], Shafi Javadi [93], Khalili et al. [94] Sabeti [95] based on different scales and systems. As for Iran's climate categorization for educational buildings, it was provided in 1989 by Kasmaei [96]. This research has not taken this categorization into account, however, since it is based only on the school year and not on the whole year that schools are used for summer tutorial activities. A recent climate classification of Iran presented by Raziei [97] is based on Köppen-Geiger Feddema and the United Nations Environment Programme (UNEP) climate classifications. Thus, this research refers to the Köppen-Geiger system as one of the most widely used climate classifications receiving increasing interest recently to study climate changes [98] and building energy/daylight analysis [9,12,99]. Based on Köppen system, Iran possesses ten types of climates (Fig. 2) in which "Bwh"(35.98%), "BSk" (23.69%), "Csa"(17.03%), "BSh" (15.70%), and "BWk"(5.94%) climates cover more than 98% of the country area. It means that Iran encompasses all arid and desert climate types of the Köppen system known as group B. Hence, to realize the research aim, considering each climate type, related cities, which are the center of their province, are selected. These cities are Yazz, Kerman, Bushehr, Mashhad, and Rasht (Table 3).

## 2.3. Case study

The case study is based on typical classrooms proposed by DRES. It consists of a single-zone educational space of 7 m(depth) × 8 m(width) × 3.5 m(height). DRES guidelines propose south- or north-window orientations to reduce energy consumption [47]. Accordingly, the case model was designed with a south-oriented double-glazed window with 3.2 U-value(W/m<sup>2</sup>K), 0.81 SHGC, and 0.76 VT, in the center of the façade wall with 45% WWR and 1.1 m sill height. Fig. 3 shows the case study characterized by heavyweight concrete walls (0.2 m thick) with brick (0.1 m thick), thermal insulation (0.05 m thick), wall air gap, and gypsum board (0.019 m thick) on the inner side and the studied shading systems. Lightweight concrete (0.1 m thick) with Acoustic tile and general ceiling air gap make up the floor, while heavyweight concrete (0.2 m thick) and brick (0.1 m thick) with insulation (0.05 m thick) make up the roof construction system (Table 4). The classroom has adiabatic common walls, while only the façade is diabatic. The input parameters for the simulation model and reflectance values of the surfaces are shown in Tables 5 and 6, respectively.

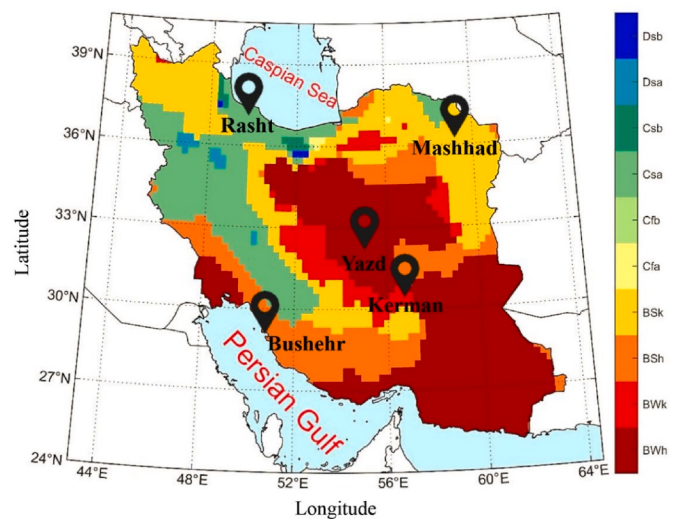


**Fig. 2.** Iran map showing Köppen climate classifications and the selected studied cities (Authors base on [97]).

**Table 3**  
Climatic parameters of selected cities, based on EnergyPlus data [100].

Weather Data	Yazd						Kerman						Bushehr						Mashhad						Rasht					
	Monthly			Monthly			Monthly			Monthly			Monthly			Monthly			Monthly			Monthly			Monthly					
	Min	Max	Average	Min	Max	Average	Min	Max	Average	Min	Max	Average	Min	Max	Average	Min	Max	Average	Min	Max	Average	Min	Max	Average	Min	Max	Average			
Dry-bulb temperature(°C)	8.23	34.69	21.08	4.50	29.47	17.35	15.98	34.05	25.69	3.34	28.92	16.178	7.72	26.42	16.75															
Relative humidity(%)	12.15	47.61	26.39	13.23	58.16	30.17	51.43	77.07	64.71	20.60	73.95	46.86	71.98	88.56	81.26															
Wind speed(m/s)	1.99	3.22	2.66	2.33	3.88	3.22	2.53	4.68	3.71	2.3125	4.402	3.190	1.49	2.06	1.78															
Direct normal radiation(W/m <sup>2</sup> )	159792	252131	210577.7	175157	253362	211968.6	162048	242131	206467.2	126771	251410	184931.3	99100	183996	137512.08															
Diffuse horizontal radiation(W/m <sup>2</sup> )	26212	61575	43382.5	26074	61624	43729.41	27964	56629	41792.08	25550	63132	43253.8	23563	64564	44432.83															
Horizontal radiation(W/m <sup>2</sup> )	106403	238809	179270.9	114964	235863	185074.3	104495	232559	176051.1	83971	239371	162237.5	64768	194169	128460															
Horizontal infrared radiation(W/m <sup>2</sup> )	245.28	353.91	295.54	251.16	326.27	274.63	315.48	410.73	357.90	242.96	332.26	289.91	293.97	391.45	338.390534															
Total sky cover(fenth)	1.06	4.37	2.75	0.82	3.83	2.40	0.0263	4.1344	1.9508	0.7656	6.1436	3.4240	4.413423	7.594631	6.362383															
Latitude, Longitude	31.89°N,54.35°E			30.28°N,57.08°E			28.91°N, 50.82°E			36.29°N,59.60°E							37.27°N,49.59°E													

### - Shadings

Shading systems in this study are fixed exterior types, including V-louver, H-louver, overhang, and egg-crate [49]. Since the light shelf has inside and outside parts, it is included in this research as well. To define the dimension range of each type of shading for optimization, an extensive literature review was conducted. Different research investigated the role of V-louver, and H-louver [25,28,36,101–103], overhang [38,68,104,105], egg-crate [106–109], light shelf [36,47, 104,110] with different depths, lengths, and angles to evaluate building daylight performance. Accordingly, the extensive dimension ranges for shading characteristics were considered (Table 7). The shading material is aluminum with 237W/mK thermal conductivity [111], 896J/kgK specific heat, 2740 kg/m<sup>3</sup> density, and infrared emittance 0.25 [112].

### 2.4. Optimization

Optimization refers to exploring and identifying the best solution(s) among miscellaneous feasible alternatives, which are the solutions satisfying all the constraints [113]. The number of criteria used to evaluate an optimization problem determines whether it is single-objective or multi-objective. Optimization with two or more goals is known as multi-objective, in contrast to optimization with only one objective [79]. Different methods can be used to solve multi-objective problems, including Weighted-Sum/Scalarization method,  $\varepsilon$ -constraints method, Goal and multi-level programming, and utility function method [113,114]. Pareto-optimal solution is the other idea to address the MOO problem. They are non-dominated solutions that cannot be dominated by other solutions.

Applying different weights for each variable, the weighted-sum method merges different goals into one single objective function. Scalarization is defined by experts as techniques, including regression models, Artificial neural networks [115], and sensitivity analysis [116].

In this research, the multi-objective optimization technique was used to find optimal design options with minimum EUI and ASE and maximum sDA. Since solar radiation impacts the building cooling/heating loads, MOO was to improve the optimal solution for all objectives:

$$F(x_1) = \min EUI \quad EUI = E_{\text{total}} (E_H + E_C + E_L + E_E) / \text{Gross floor area} \quad (5)$$

$$F(x_2) = \min (\text{ASE})$$

$$F(x_3) = \max (\text{sDA})$$

Where  $E_H$  indicates heating energy,  $E_C$  is energy demand for cooling, and  $E_L$  and  $E_E$  refer to lighting and equipment energy, respectively.

The algorithm based on the dimensions and features of window, and the studied shading systems was identified. The applied parameters in this study are dimensions and angles of FESSs as well as WWR(Table 7). The range value for shading depth is changed at 0.1 m and for the angle at 10-degree intervals.

The study begins by investigating Pareto-front to explore optimal solutions. Accordingly, Pareto solutions with the best EUI, sDA, and ASE, as well as the balanced option for each climate zone and applied shading system, were recommended. Second, to accurately define the absolute optimum solution within Pareto-fronts, the weighted-sum method applied by previous research [28,79,117] was conducted in Excel. Using the fitness function (Section 2.1 Simulation), the function value of each model is examined, and for each objective, the absolute optimum genome is explored.

Applying different weights for each variable, the weighted-sum method merges different goals into one single objective function. This method can be expressed as [118]:

$$F(x) = w_1 f_1(x) + w_2 f_2(x) + \dots + w_M f_M(x)$$

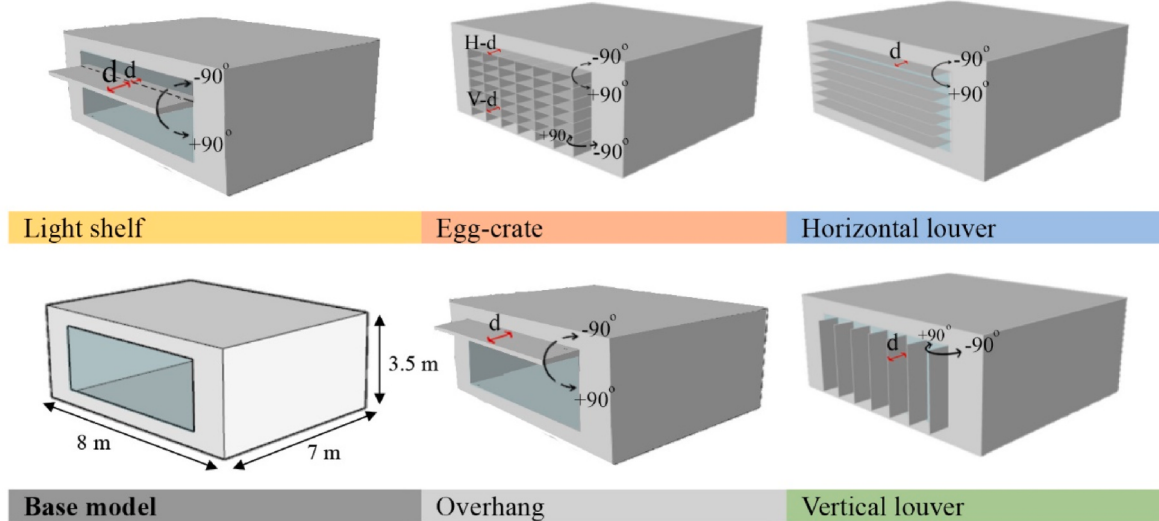


Fig. 3. Exterior shading systems, their studied variables, and the base model.

**Table 4**  
Thermal properties of the model materials.

Construction		Conductivity(W/mK)	Density(kg/m <sup>3</sup> )	Specific heat(J/kgK)	U-Factor (W/m <sup>2</sup> K)	R-Value (m <sup>2</sup> .K/W)
Roof	Brick	0.889	1920.004	789.490	0.481527	1.912975
	Heavyweight concrete	1.948	2240.005	899.419		
	Insulation board	0.029	43.0	1209.219		
Wall	Brick	0.889	1920.004	789.490	0.426351	2.18173
	Heavyweight concrete	1.948	2240.005	899.419		
	Insulation board	0.029	43.0	1209.219		
	Generic Wall Air Gap	0.667	1.28	1000.0		
Floor	Gypsum board	0.159	800.001	1089.297		
	Acoustic tile	0.059	368.0	589.619	1.170985	0.690229

**Table 5**  
The input parameters for the simulation model.

Parameters	value
Occupied period	8–18
Cooling setpoints	26 °C
Heating setpoint	20 °C
Daylight Illuminance setpoint	500 Lux
Number of people per unit of area	0.35 ppl/m <sup>2</sup>
Infiltration rate per area*	0.0003 m <sup>3</sup> /s·m <sup>2</sup>
*According to ASHRAE recommendation for Average building (0.5 cfm/ft <sup>2</sup> at 75Pa corresponds to 0.0003 m <sup>3</sup> /s·m <sup>2</sup> at 4Pa)	

**Table 7**  
Ranges of shading characteristics.

Variable	Ranges	
	Depth	Tilt angle
V-louver	0.1–1 m	0≤θ(°)≤180
H-louver	0.1–1 m	0≤θ(°)≤180
Egg-crate	Horizontal depth:0.1–1 m Vertical depth:0.1–1 m	0≤θ(°)≤180
Light shelf	Exterior depth: 0.1–1 m Interior depth: 0.1–0.5 m	0≤θ(°)≤180
Overhang	0.1–2 m	0≤θ(°)≤180
WWR	10%–90%	

**Table 6**  
Reflectance values of model surfaces for simulation.

Model structure	Value
Interior surfaces	Wall Ceiling Floor
exterior surfaces	Shading types Earth surface
	50% 70% 20% 80% 20%

Accordingly, the solution is highly dependent on the weighting coefficient  $w=(w_1, \dots, w_M)$ , which is positive, satisfying

$$\sum_{i=1}^M w_i = 1, \quad w_i \in (0, 1)$$

In this research, weighted-sum method can be stated as:

$$FF_i = (sDA_i - sDA_{min})C_1 - (ASE_i - ASE_{min})C_2 - (EUI_i - EUI_{min})C_3 \quad (6)$$

Where  $i$  is the iteration result and  $\min$ , and  $\max$  are the minimum and maximum values of optimization sets, respectively.

$$C_1 = 100/sDA_{max} - sDA_{min} \quad (7)$$

$$C_2 = 100/ASE_{max} - ASE_{min} \quad (8)$$

$$C_3 = 100/EUI_{max} - EUI_{min} \quad (9)$$

Where, min/max values show the minimum/maximum values of each objective within the solutions found by the optimization algorithm.

Octopus a Grasshopper plugin, was applied for MOO. This plugin has been drastically popular, especially in the field of building performance optimization [25,31,79,119], and was verified by Refs. [120–122]. To realize MOO, Octopus performs based on Strength Pareto Evolutionary Algorithm (SPEA-2) in association with the Hypervolume Estimation Algorithm (HypE) , an innovative hypervolume-based multi-objective

evolutionary algorithm applied in terms of its advantages compared to other multi-objective optimization techniques [123]. Because of its attractive theoretical properties, hypervolume is considered one of the most popular second-level sorting criteria. The hypervolume indicator of  $S$  is the measure of region dominated by  $S$  and restricted above by  $r$ , when point set  $S \subset R^d$  and reference point  $r \in R^d$  [124]

$$H(S) = \Lambda(\{q \in R^d \mid \exists p \in S : p \leq q \text{ and } q \leq r\}) \quad (10)$$

Where  $\Lambda(\cdot)$  denotes the Lebesgue measure. A point  $p \in R^d$  is said to weakly dominate a point  $q \in R^d$  if  $p_i \leq q_i$  for all  $X^* = \{(p_x, p_y), (q_x, q_y)\}$ .

Inspired by evolution principles in nature, Octopus improves the population of solutions by selection, crossover, and mutation [25]. The values for Elitism, Mutation probability, Mutation rate, population size of the first generation, and Crossover rate are determined as 0.5, 0.2, 0.9, 100, and 0.8, respectively.

To realize the research objective, 25 optimizations were conducted for five studied shading systems in five different climate zones. The possible solutions for each shading type, including V-louver, H-louver, egg-crates, light shelf, and overhang are 1710, 1710, 34200, 8550, and 3591, respectively, and sequentially. The total possible design options for each climate zone regarding five FESSs are 49761. There was a total of 248,805 feasible design options taken into account, considering all climate zones and shading types. A total of 746,415 simulations are required to assess and enhance the model's daylight and energy metrics. The Pareto optimal solutions' objective performances were compared to the basic model's, using the determined attributes (Table 8).

### 3. Results

Here, the results of a model's parametric optimization of daylight and energy performances are presented. First, it begins by analyzing the results of Pareto solutions, and then the best optimal solutions across all climatic zones are examined. Last but not least, sensitivity analysis was used to investigate the connection between design factors and performance objectives.

#### 3.1. Pareto frontiers solutions

**Fig. 4** presents the scatterplots of simulated models, and the related performance metrics. Besides, to evaluate and visualize the design options as well as the Pareto fronts explicitly, the TT toolbox, Colibri [125], and Design Explorer [126] were used to illustrate the relationship among studied design variables and the performance metrics presented in the Supplementary material. The values of the performance metrics and the characteristics of the Pareto fronts, are presented in Table 8, as well. Since some design options in each city have the same value for one performance metric, one design solution has been selected randomly to be presented. The results are as follows:

- In Yazd(BW), the highest ASE (0%) happens in all shading types except for the light shelf with 1.2% ASE. Hence, they can meet the LEED requirement compared to the base model with an ASE value of 38.1%. WWR for the model with the best ASE in V-louver, light shelf, and overhang is 10%, while in H-louver and egg-crates is 40%. Besides, the best sDA level, 100%, is the same as the sDA for the base model, for V-louver, H-louver, light shelf, and overhang, with 40%, 60%, 40%, and 30% WWR, respectively. In contrast, egg-crates has 98.80% sDA within 40% WWR. With 20% WWR, the EUI for V-louver is the lowest at 36.80%. Egg-crates, overhangs, light shelves, and H-louvers with 10% WWR have energy improvements of 27.65%, 27.54%, 26.81%, and 23.05%, respectively, and in that order. In general, all selected Pareto front design options surpass the energy performance of the base mode by 171.28 kWh/m<sup>2</sup>/yr EUI and meet the LEED requirement for ASE and sDA.

- In Kerman (BWk), ASE is met with the optimum value of 0% for all FESS with 10% WWR except for H-louver (20%WWR), compared to the base model with 33.3% ASE. Besides, egg-crates, light shelf, and H-louver, all with 40% WWR, provide 100% sDA for the studied classroom, while V-louver (20%WWR) provides 71.42% ASE and still can pass the LEED standards for daylight. No Pareto optimum with an overhang can satisfy this requirement since the highest sDA value is 42.2619% for a window with 10% WWR. The lowest EUI is dedicated to the overhang-installed model with 102.976 kWh/m<sup>2</sup>/yr, followed by light shelf and egg-crates with 103.075 and 105.01 kWh/m<sup>2</sup>/yr EUI, all with 10% WWR, and H-louver and V-louver with 106.746 and 107.093 kWh/m<sup>2</sup>/yr EUI, respectively, and with 20% WWR. In general, maximum EUI improvement of 22.79%, 22.72%, 21.27%, 19.97%, and 19.71% over the reference model is dedicated to the design options with overhang, light shelf, egg-crates, H-louver, and V-louver, respectively.
- In Bushehr (BSh), all selected Pareto optimums and the base model achieve an ASE of 0%. Accordingly, WWR for the egg-crates, overhang, and H-louver is 20%, while that of the V-louver and light shelf are 60% and 10%, in order. In terms of sDA, the same as the base model, H-louver with 40% and light shelf with 30% provide 100% sDA. The second, third, and fourth ranks belong to V-louver (30% WWR) with 99.40%, overhang (30% WWR) with 98.80%, and egg-crates (40% WWR) with 83.33% sDA level. Regarding energy performance, energy saving belongs to the models with 10% WWR with any type of shading device and outperforms the base model with 332.44 kWh/m<sup>2</sup>/yr EUI. Meanwhile, the highest and lowest energy efficiency is related to egg-crates and H-louver with 24.47% and 22.27% energy improvement, respectively. Overhang, V-louver, and light shelf, with the maximum energy use improvement of 23.82%, 22.82%, 22.70%, and EUI values of 253.224, 256.548, and 256.944 kWh/m<sup>2</sup>/yr are the second, third and fourth optimum design options. In general, all of the design options with the best performance metrics meet the building's energy needs and satisfy daylighting criteria.
- In Mashhad (BSk), all FESS-integrated models outperform the base model where ASE<sub>1000,250</sub> is received for 41.7% occupied area. The optimum ASE value in shading devices including egg-crates and H-louver with 20% WWR as well as the light shelf with 10% WWR is 0%. In contrast, the minimum ASE in the V-louver and overhang models is 0.6% and 3.6%, respectively with 10%WWR. Besides, sDA level for all shading types, including H-louver (50% WWR), light shelf (40%WWR), overhang(10%WWR), egg-crates(70%WWR), and the base model is 100% while V-louver (30% WWR) has the lowest sDA level by 99.40%. Within the Pareto solutions, the highest and lowest EUI is dedicated to the models with V-louver (20%WWR), and overhang (10%WWR) by 17.14% and 20.48% energy saving compared to the base model by 131.944 kWh/m<sup>2</sup>/yr EUI. Besides, light shelf (10%WWR), H-louver (20%WWR), and egg-crates (10% WWR) stand at the second, third, and fourth places via contribution to energy efficiency by 20.48%, 18.08%, and 18.00%, respectively. Generally, except for the sDA, all Pareto designs improved the ASE and EUI of the base model through MOO processes.
- In Rasht (Csa), no more than 10% of the workspace received ASE<sub>1000,250</sub> in all simulated models and outperformed the base model with 44% ASE. Meanwhile, only overhang-installed model (10% WWR) has 3% ASE. WWR parameters of the V-louver, light shelf, and egg crate are 20%, while that of H-louver is 40%. Only overhang by 36.30% value cannot achieve sufficient sDA level, although H-louver (40%WWR), light shelf(50%WWR), and egg-crates(90%WWR) with 100% as well as V-louver (30%WWR) with 87.5% sDA level can meet LEED requirement for daylight metrics. The EUI findings show that every Pareto front contributes to the model's energy efficiency. By implementing overhang, light shelf, H-louver, V-louver, and egg-crates, the classroom's energy efficiency increases by 16.52%, 16.28%, 14.31%, 13.67%, and 12.69%, respectively.

**Table 8**

Pareto optimal solutions, including design options with the best EUI, the best sDA, the best ASE, and the base model.

City	Variable	Vertical Louver			Horizontal Louver			Light-shelf			Overhang			Egg-crater			Base-model			
		ASE (%)	sDA(%)	EUI (kWh/m <sup>2</sup> /yr)	ASE (%)	sDA(%)	EUI (kWh/m <sup>2</sup> /yr)	ASE (%)	sDA(%)	EUI (kWh/m <sup>2</sup> /yr)	ASE (%)	sDA(%)	EUI (kWh/m <sup>2</sup> /yr)	ASE (%)	sDA(%)	EUI (kWh/m <sup>2</sup> /yr)	ASE (%)	sDA(%)	EUI (kWh/m <sup>2</sup> /yr)	
Yazd	WWR (%)	0	100	108.234	0	100	131.796	1.2	100	125.347	0	100	124.107	0	98.8095	123.909	38.1	100	171.28	
	Depth (m)	10	40	20	40	60	10	10	40	10	10	30	10	40	40	10				
	Angle (°)	0.7	0.2	0.2	0.5	0.3	0.5	In* = 0.3 Ex** = 1	In = 0.5 Ex = 0.7	= 0.4	0.8	0.8	0.8	V*** = 0.5 H**** = 0.5	V = 0.1 H = 0.5	V = 0.2 H = 0.3				
	WWR (%)	0	71.4286	107.093	0	100	106.746	0	100	103.075	0	100	42.2619	102.976	0	100	105.01	33.3	100	133.383
	Depth (m)	10	20	20	20	40	20	10	40	10	10	10	10	10	40	10				
	Angle (°)	0.6	0.1	0.1	0.3	0.3	0.1	In = 0.4 Ex = 1	In = 0.4 Ex = 0.7	= 20	0.9	0.9	0.9	V = 0.4 H = 0.5	V = 0.1 H = 0.4	V = 0.1 H = 0.4				
Kerman	WWR (%)	0	99.4048	256.548	0	100	258.383	0	100	256.944	0	98.8095	253.224	0	83.3333	251.091	32.7	100	332.44	
	Depth (m)	60	30	10	20	40	10	10	30	10	20%	30	10	20	40	10				
	Angle (°)	0.8	0.1	0.2	0.3	0.2	0.4	In = 0.2 Ex = 0.9	In = 0.3 Ex = 1	= 0.1	1	1	0.8	V = 0.2 H = 0.3	V = 0.2 H = 0.3	V = 0.2 H = 0.9				
	WWR (%)	60	20	0	30	30	0	-80	10	40	70	20	0	V = -30 H = 10	V = -30 H = 10	V = -30 H = 0				
	Depth (m)	0.8	0.1	0.2	0.3	0.2	0.4	In = 0.2 Ex = 0.9	In = 0.3 Ex = 1	= 0.1	1	1	0.8	V = 0.2 H = 0.3	V = 0.2 H = 0.3	V = 0.2 H = 0.9				
	Angle (°)	60	20	0	30	30	0	-80	10	40	70	20	0	V = -30 H = 10	V = -30 H = 10	V = -30 H = -10				
Bushehr	WWR (%)	0	99.4048	109.325	0	100	108.085	0	100	105.655	3.6	100	104.911	0	100	108.185	41.7	100	131.944	
	Depth (m)	10	30	20	20	50	20	10	40	10	10	10	10	20	70	10				
	Angle (°)	0.6	0.1	0.2	0.3	0.3	0.1	In = 0.4 Ex = 0.9	In = 0.3 Ex = 1	= 0.1	1	1	0.8	V = 0.1 H = 0.6	V = 0.5 H = 0.6	V = 0.1 H = 0.2				
	WWR (%)	0.6	99.4048	126.488	0	100	125.546	0	100	122.669	3	36.3095	122.321	0	100	127.927	44	100	146.528	
	Depth (m)	10	30	30	40	40	20	20	50	10	10	10	10	20	90	10				
	Angle (°)	-20	-40	0	30	30	-30	-70	0	10	50	20	-20	V = 40 H = 0	V = 0 H = 10	V = -30 H = 10				
Rasht	WWR (%)	0	87.5	126.488	0	100	125.546	0	100	122.669	3	36.3095	122.321	0	100	127.927	44	100	146.528	
	Depth (m)	20	30	30	40	40	20	20	50	10	10	10	10	20	90	10				
	Angle (°)	1	0.2	0.2	0.5	0.2	0.1	In = 0.3 Ex = 0.9	In = 0.3 Ex = 1	= 0.3	0.7	1	1	V = 0.7 H = 1	V = 0.2 H = 0.3	V = 0.5 H = 0.3				
	WWR (%)	-80	0	0	10	10	-50	70	40	20	40	-30	-30	V = 30 H = -50	V = 0 H = 20	V = -40 H = -20				
	Depth (m)	-80	0	0	10	10	-50	70	40	20	40	-30	-30	V = 30 H = -50	V = 0 H = 20	V = -40 H = -20				
	Angle (°)	-80	0	0	10	10	-50	70	40	20	40	-30	-30	V = 30 H = -50	V = 0 H = 20	V = -40 H = -20				

\*Interior \*\*Exterior \*\*\*Vertical \*\*\*\*Horizontal.

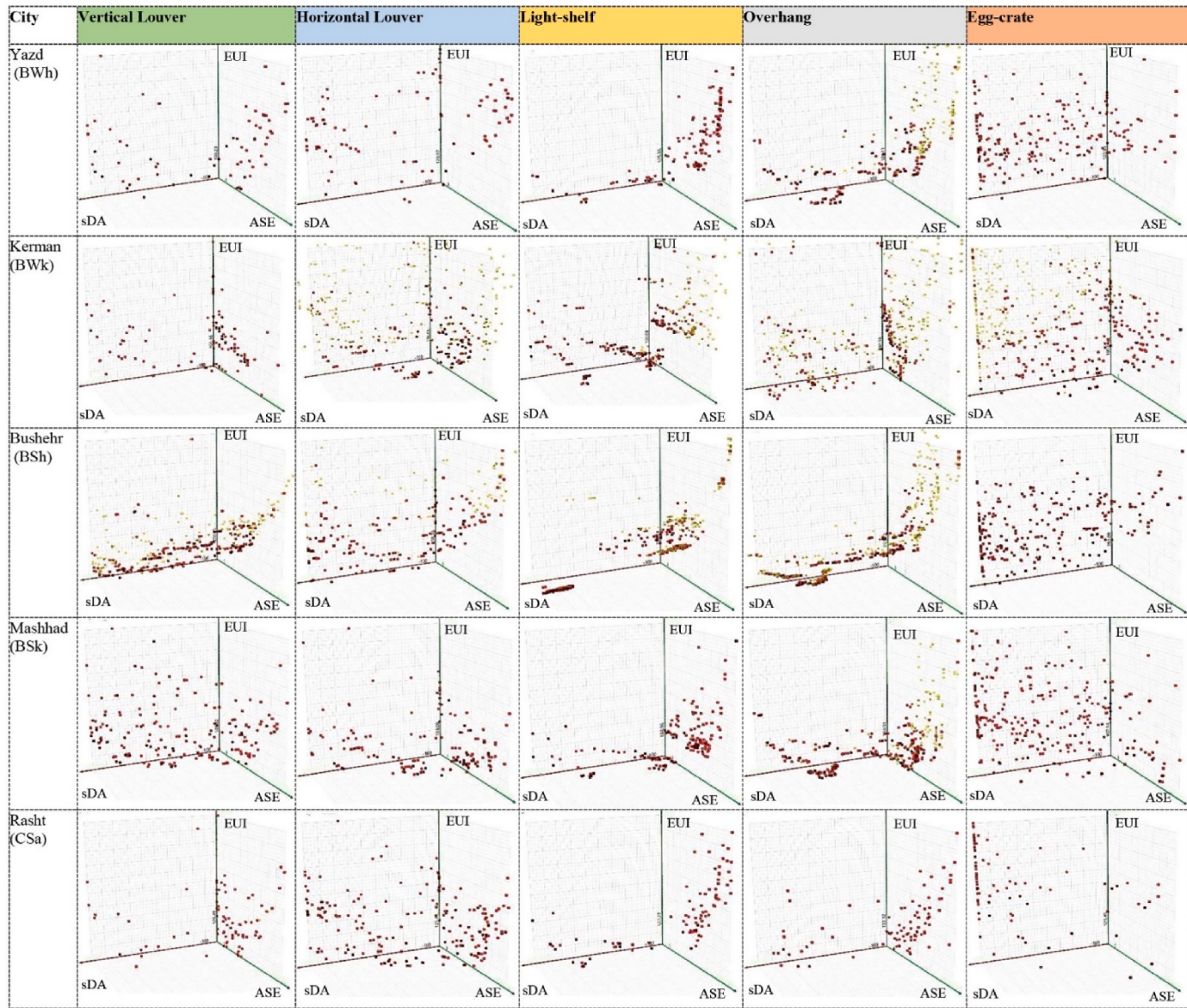


**Fig. 4.** Scatterplot illustrating EUI, sDA, and ASE of the simulated models.

### 3.2. Absolute optimum solution

Table 9 presents the absolute optimum solutions derived from Pareto fronts (Section 2.4) via the optimization process in the five studied climate zones. Besides, Fig. 6 illustrates the improvement/decrease of energy and daylight performance of the absolute optimum solutions compared to the base model. The results of this part of optimization are as follows:

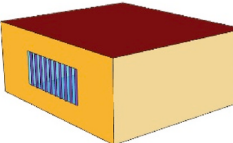
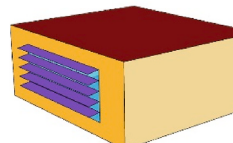
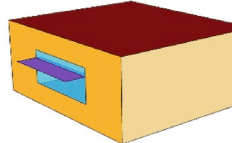
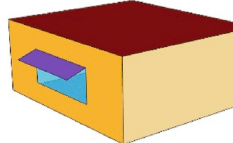
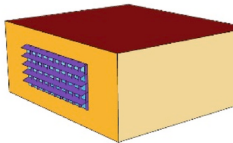
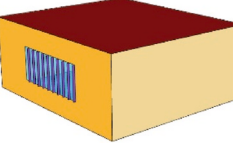
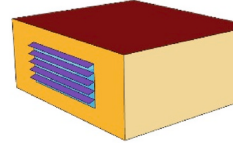
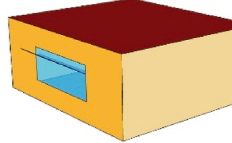
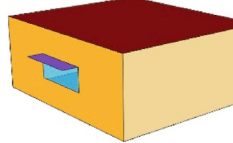
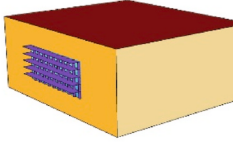
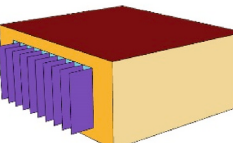
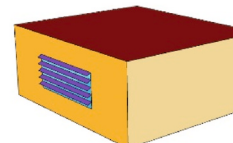
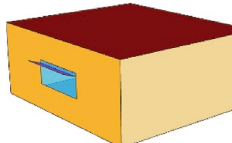
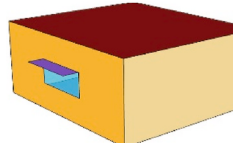
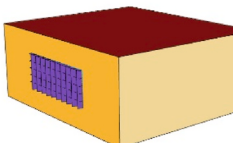
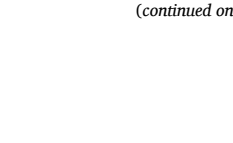
- In Yazd (BWh), all optimum genomes provide the standard level of sDA and ASE (Fig. 5). Although all solutions enhance ASE, they reduce sDA values. The daylight performance of H-louver-installed model surpasses the other systems by 0%ASE, and 60.119% sDA values with 40%WWR, 0.5depth, and 10° angle. However, its contribution to the energy efficiency of the model is the lowest by 18.59% EUI improvement. The highest energy performance is dedicated to V-louver-installed model with 20%WWR, 0.1depth, and 60° angle, with 36.72% energy-saving. Furthermore, overhang, light shelf, and egg crate stand at second, third, and fourth ranks by 24.33%, 23.98%, and 22.50% in energy saving, respectively. The

range of WWR of the FESS-integrated building in hot desert climates is between 20% and 40%.

- In Kerman (BWk), similar to Yazd, the H-louver-installed model has the best daylight performance with 0% ASE and 91.07% sDA. With an energy consumption of 112.351 kWh/m<sup>2</sup>/yr, it is likewise considered the highest energy demand model. This indicates a negative correlation between daylight and energy metrics. Among all shadings, the egg-crane and overhang cannot meet the LEED requirement for daylight metrics. Although ASE for the first and the latter are 0% and 4.2%, their sDA level are 49.40% and 33.92%, respectively. However, overhang has the most significant role in reducing EUI by 22.31%, followed by V-louver, Egg-crane, light shelf, and H-louver by 19.71%, 19.52%, 18.41%, and 15.77%, in order.
- In Bushehr (BSh), only V-louver, overhang, and H-louver can achieve the daylight standards by ASE and sDA values of 2.4%, 92.26%, 3, 63.69% and 0, 52.38%, correspondingly. While light shelf by 19.64% and egg-crane by 40.47% sDA cannot pass the standard levels; however, they considerably reduce ASE level compared to the base model by 92.66% and 100%, respectively. The same as Yazd and Kerman, a high level of sDA in Bushehr is accompanied by high

**Table 9**

Variables and performance metrics of absolute optimum solutions.

	Vertical louver			Horizontal louver			Light shelf			Overhang			Egg-crate		
	ASE(%)	sDA(%)	EUI (kWh/m <sup>2</sup> /yr)	ASE(%)	sDA(%)	EUI (kWh/m <sup>2</sup> /yr)	ASE(%)	sDA(%)	EUI (kWh/m <sup>2</sup> /yr)	ASE(%)	sDA(%)	EUI (kWh/m <sup>2</sup> /yr)	ASE(%)	sDA(%)	EUI (kWh/m <sup>2</sup> /yr)
<b>Yazd</b>															
WWR(%)	7.1	60.119	108.383	0	100	139.435	4.8	86.3095	130.208	6	76.1905	129.613	2.4	83.33	132.73
Depth(m)	20			40			20			20			30		
Angle( <sup>o</sup> )	0.1			0.5			In* = 0.2, Ex** = 0.9			0.9			V*** = 0.1, H**** = 0.3		
	60			10			0			20			V = 50, H = 20		
															
<b>Kerman</b>															
WWR(%)	6	71.42	107.093	0	91.071	112.351	0.6	67.261	108.829	4.2	33.928	103.621	0	49.404	107.341
Depth(m)	20			30			20			10			20		
Angle( <sup>o</sup> )	0.1			0.3			In = 0.2, Ex = 0.8			0.7			V = 0.1, H = 0.4		
	10			20			-30			0			V = -40, H = 0		
															
<b>Bushehr</b>															
WWR(%)	2.4	92.261	281.696	0	52.381	258.73	2.4	19.642	257.44	3	63.690	261.21	0	40.476	256.69
Depth(m)	50			20			10			20			20		
Angle( <sup>o</sup> )	1			0.2			In = 0.2, Ex = 0.6			1			V = 0.2, H = 0.3		
	0			30			-20			30			V = -30, H = 10		
															
<b>Mashhad</b>															
WWR(%)	7.7	82.738	117.758	0	86.904	114.98	6	80.357	109.177	7.1	100	109.474	0	93.452	119.444
Depth(m)	40			30			20			10			40		
Angle( <sup>o</sup> )	0.8			0.5			In = 0.2, Ex = 0.8			0.6			V = 0.1, H = 0.6		
	-10			0			-10			20			V = 40, H = 0		
															

(continued on next page)

Table 9 (continued)

	Vertical louver			Horizontal louver			Light shelf			Overhang			Egg-crater		
	ASE(%)	sDA(%)	EUI (kWh/m <sup>2</sup> /yr)	ASE(%)	sDA(%)	EUI (kWh/m <sup>2</sup> /yr)	ASE(%)	sDA(%)	EUI (kWh/m <sup>2</sup> /yr)	ASE(%)	sDA(%)	EUI (kWh/m <sup>2</sup> /yr)	ASE(%)	sDA(%)	EUI (kWh/m <sup>2</sup> /yr)
Rasht	15.5	87.5	126.488	6.5	100	128.919	5.4	58.333	126.389	12.5	36.309	122.321	10.7	33.92	125.446
	WWR(%)	30	0.2	30	0.7	-10	20	In = 0.3, Ex = 0.7	-20	10	1	-30	30	V = 0.6, H = 0.4	V = -10, H = -30
	Depth(m)														
	Angle( $^{\circ}$ )														

\*In=Interior \*\*Ex=Exterior \*\*\*V=Vertical \*\*\*\*H=Horizontal.

\*In=Interior \*\*Ex=Exterior \*\*\*V=Vertical \*\*\*\*H=Horizontal.

energy consumption. As a result, the model with the egg-crater has the maximum energy efficiency at 22.78%, while the model with the V-louver has the lowest energy efficiency at 15.26%. In hot, semi-arid climate, WWR might be higher to achieve optimization objectives than in Yazd and Kerman. This range is between 10 and 50%.

- In Mashhad (BSk), contrary to Bushehr and Kerman and the same as Yazd, all the absolute optimum solutions meet the daylight standards for sDA and ASE. The highest sDA level is 100% provided by overhang, and the lowest belongs to the light shelf at 80.35%. Besides the highest and lowest ASE is for V-louver by 7.7%, and H-louver and egg-crater by 0%, which results in a 100% ASE reduction. Among FESSs, egg crate has the least contribution to energy saving by 9.47%, while the highest is dedicated to the light shelf by 17.26%. Moreover, the light shelf has the lowest sDA and EUI, the same as the overhang in Kerman and the V-louver in Yazd. Notwithstanding, the energy consumption of the base model was decreased by applying any kind of FESS through optimization. The optimization also presents that in cold-semi arid climate WWR ratio between 10 and 40% potentially can accomplish lower EUI and ASE as well as higher sDA levels.
- In Rasht (Csa), only V-louver, H-louver, and light shelf can achieve acceptable levels of daylight metric by 15.5%, 6.5%, and 5.4%, ASE and 87.5%, 100%, and 58.33 sDA values, respectively and sequentially. Meanwhile, H-louver has the lowest energy-saving by 12.02%, and overhang outperforms all systems by 16.52% EUI reduction. The ranges of WWR in Kerman's dry arid environment (10–30%) are identical to those in the hot-summer Mediterranean climate. But in Rasht, H-louver, V-louver, and egg-crater may all have 30% WWR, but only the Kerman model with the H-louver has 30% WWR.
- The ranges of vertical and horizontal depths, as well as proposed WWR of egg crates in Pareto solutions, are between 0.1 and 0.6 m, 0.3–0.6 m, and 20–40%, in five climate zones, respectively. The deepest V-louver should be applied in Rasht with 0.6 m and  $-10^{\circ}$  angles, and the lowest depth, 0.1 m, can be used in Yazd with  $50^{\circ}$ , Kerman with  $-40^{\circ}$ , and Mashhad with  $40^{\circ}$  angles. Besides, the deepest H-louver belongs to Mashhad with 0.4 m and  $0^{\circ}$ , and the lowest depth, 0.3 m, should be applied in Yazd and Bushehr with 20 and  $10^{\circ}$  angle, respectively. Aside from daylight and energy efficiency, it should be remembered that building an eggcrate with varying depths and angles is a difficult undertaking, and designers should take into account the aesthetic effects of their design.
- Overhang plays the most considerable role in reducing energy demands in Yazd with 0.9 m depth and  $20^{\circ}$  angle. However, it has the most inferior role in Rasht with 1 m and  $-30^{\circ}$  depth and angle, respectively, both with 30%WWR. This can be due to the significant role of solar radiation control in hot desert climates to reduce building energy demands.
- Light shelf-installed model has the most efficient daylight, and energy performance in Yazd, with the highest sDA and lowest EUI value compared to the other climate zones. In Bushehr, with the lowest latitude and high humidity, sDA level in this model is very low, while EUI stands at the second rank after Yazd. WWR of Pareto optimum models in all climates is defined as 20% except for Bushehr with 10% WWR. Considering shading characteristics, Yazd, where sun radiation control is a critical issue in regulating energy and daylight metrics, has the greatest exterior shading length equal to 0.9 m. Bushehr has the smallest exterior depth of 0.6 m, followed by Rasht with 0.7 m, which is less exposed to direct sunlight owing to the high humidity in the region. The inner depth of shade in all climates is 0.2 m, with the exception of Rasht, which has a depth of 0.1 mm.
- H-louver beats other FESSs in terms of daylight metrics, as mentioned above. The ranges of WWR, depth, and angle are defined between 30 and 40%, 0.2–0.7 m, and 10–30% in the models. In Bushehr, H-louver has the highest energy efficiency and the lowest sDA level compared to the other climates. However, it performs

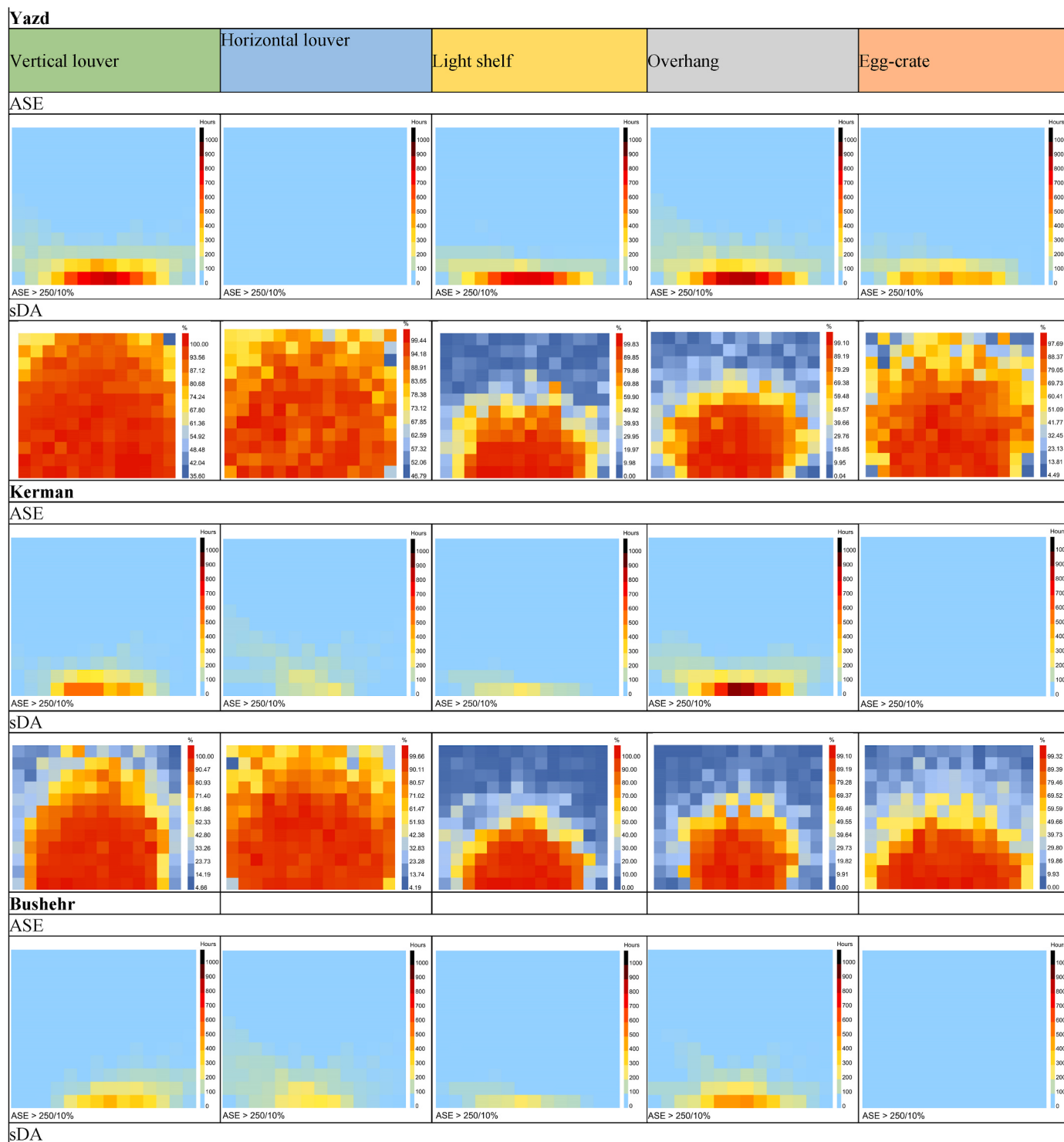


**Fig. 5.** Daylight performance of the absolute design solutions.

perfectly by reducing 100% ASE in all climate zones except for Rasht by 85.23% ASE reduction, which still meets the standards.

- V-louver has the weakest performance to control ASE metric compared to the other shading systems, especially in Rasht with 64.77% ASE value. However, its role in meeting sDA acceptable level stands at the second rank after H-louver. It also has the most considerable role in reducing EUI in Yazd, with the lowest depth of 0.1 m showing its great performance in reducing the cooling load in

hot-desert climates. The ranges of WWR, depth, and angle of the Pareto optimum solution with H-louver are between 20 and 30%, 0.1–1 m, and  $-60$  to  $10^{\circ}$ .

#### 4. Sensitivity analysis

Helping to study the significance of the variables, sensitivity analysis, as a validated tool, identifies the relationship between design

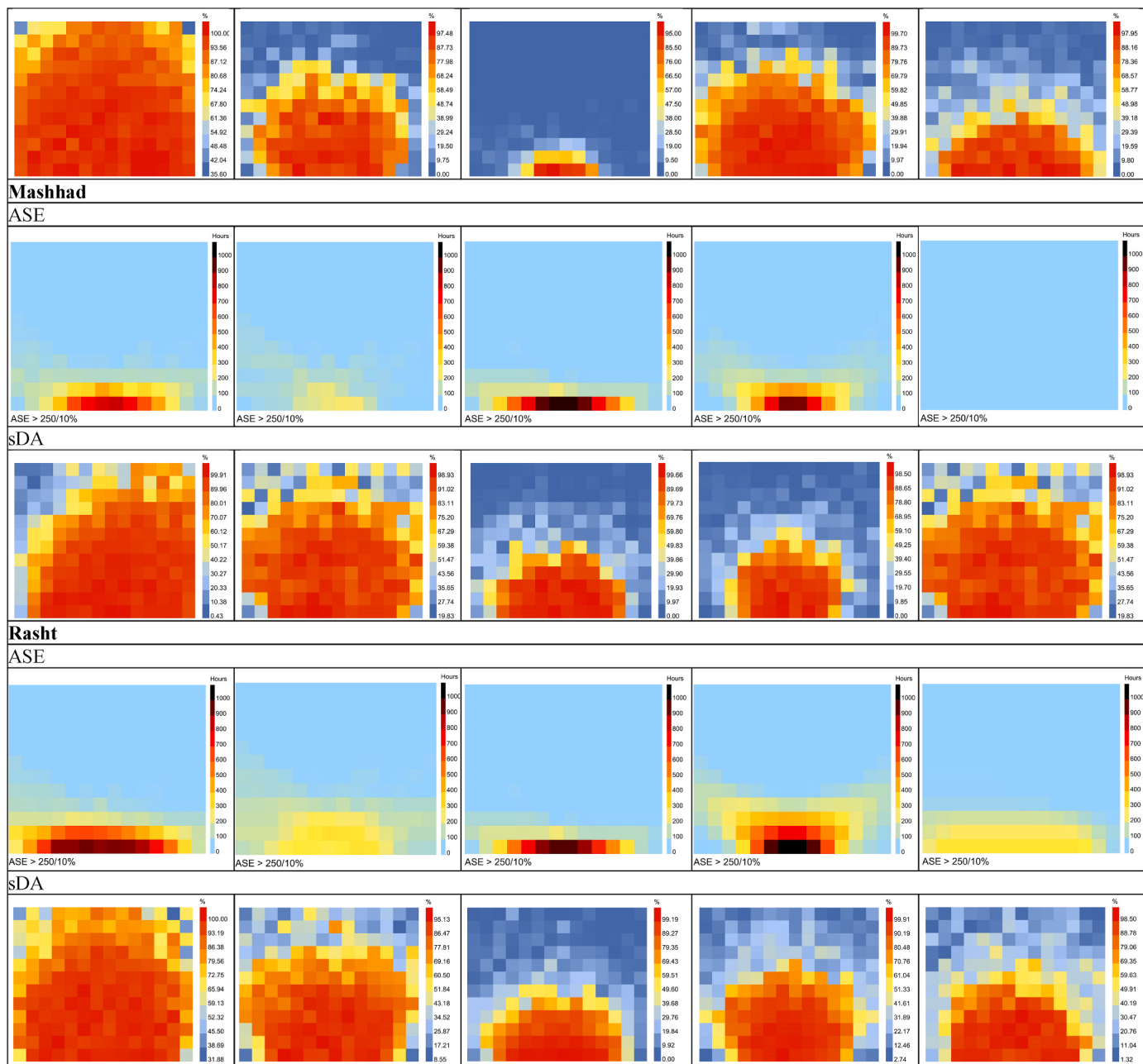


Fig. 5. (continued).

variables and performance metrics [127]. In this research, sensitivity analysis, a common method in building energy research, is used to investigate the relative impact of design variables, including WWR and shading features, on the educational building performance metrics ASE, sDA, and UDI. Thus, the statistical technique, the multiple linear regression (MLR) using Standardized Regression Coefficients(SRC) and Unstandardized Regression Coefficient(USRC), were applied as unitless and real-life scale indices of sensitivity analysis methods, respectively. SRC absolute value indicates the magnitude, while positive/negative coefficients are signs of a positive/negative relationship between the variable and performance metrics. According to the results (Fig. 7):

- In Yazd, WWR has the strongest positive effect on sDA and EUI, considering all shading types excluding V-louver, whose depth affects the indices the most. Therefore, WWR in the V-louver-integrated façade has the highest SRC value in relationship with ASE. Horizontal depth of the egg-crates, angle of overhang, exterior depth

of the light shelf, and depth of H-louver by 0.984, -0.961, 0.727, and -0.822 have the greatest positive and negative impact on ASE, respectively.

- In Bushehr, the same as Yazd, the most prominent parameter affecting sDA and EUI is WWR, except for egg-crates whose horizontal depth has the highest effect by -0.731. WWR in light shelf- and V-louver-integrated façade have the highest impact on ASE, while the lowest impact is dedicated to egg-crates.
- In Kerman, WWR has the highest influence on sDA and EUI. It also has the lowest SRC value across all performance metrics for the overhang-installed model. Horizontal angles of egg-crates and overhang, positively and light shelf, negatively affect ASE. Furthermore, the depths of the H-louver and V-louver show the largest positive connection with ASE.
- In Mashhad, sDA is considerably affected by WWR in all shadings, positively. However, only in egg-crates and V-louver, this variable has the highest SRC value in relation to EUI. The angle of the light shelf

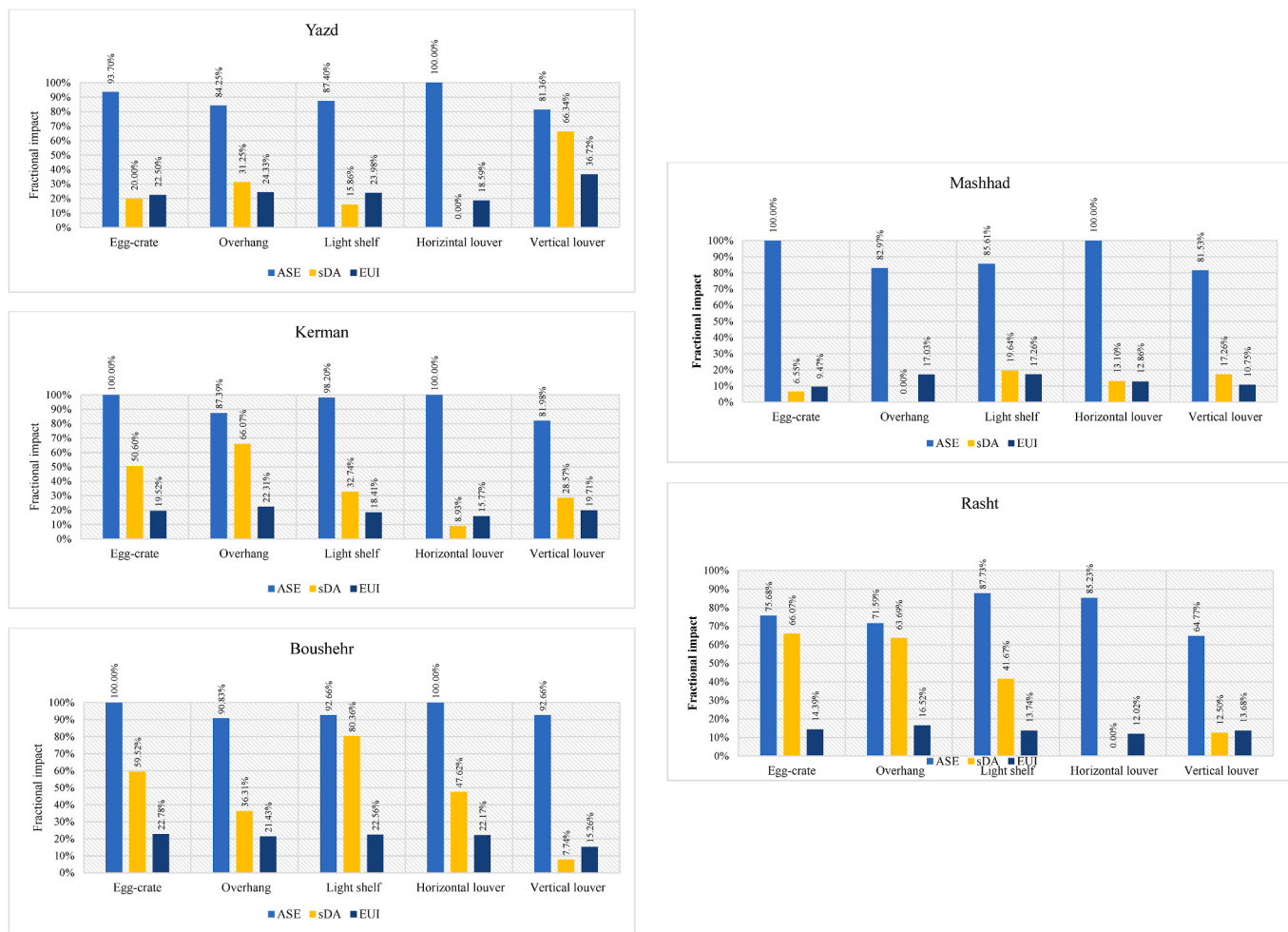


**Fig. 6.** Fractional impact of energy, and daylight performance of the absolute optimum solutions compared to the base model.

and overhang, the vertical depth of the egg-crate, along with the depth of the H-louver and V-louver also possess greater SRC magnitude in relation to ASE.

- In Rasht, WWR still stands at the first rank by a positive correlation with sDA in all shadings, except for overhang, whose angle plays the most considerable role. WWR has the lowest effect on EUI in the overhang and V-louver, while it has the highest impact in the H-louver-installed model. Concerning ASE, the vertical depth of egg-crate, angle of overhang, and depth of V-louver have the greatest negative SRC, while the angle of the light shelf and WWR in H-louver have the greatest positive SRC values.

## 5. Validation

Using the comparison method, the results validation was conducted to evaluate the accuracy of the results of building performance simulator. Honeybee versions 0.0.64 and 0.0.69 for the old Legacy plugin were validated by previous studies [86,120,128]. In this research, the results of the new version of Honeybee for Ladybug Tools 1.6.0 were verified by comparing them to the validated example case No.600 (BESTest) in the ANSI/ASHRAE Standard 140-2020 (Fig. 8). Thus, it is concluded that simulation results by Honeybee could achieve sample test(case 600) validation, and it is in accordance with ASHRAE Standard 140-2020(Figs. 9–11).

## 6. Discussion

This research presents a MOO framework for shading-based passive

design strategies in the early-stage design of a sustainability-oriented educational building.

Different research studied the optimization role in building sustainable performance improvement and revealed the significance of MOO to enhance more than one objective metric in combination with different parameters. Using expanded-metal shading, Khidmat et al. [19] met LEED v4.1 daylight requirements by 100% ASE reduction and about 50% UDI improvement compared to the base model through the MOO approach. Wang et al. [130] proposed MOO framework for the classroom external shading system, resulted in reducing 4.5%–18.8% total EUI and at least 27% window solar irradiance, as well as 25%–37% lighting quality, and more than 30%, visual comfort improvement. Ebrahimi-Moghadam et al. [36] could achieve 9.44%, 19.17%, and 11.38% energy saving in residential building's total cooling, heating, and electrical load, respectively by using light shelves.

By comparing the sustainability-oriented performances of a school building envelope integrated with five different shading systems and comparing their potential in energy and daylight performance metrics in five different climates, this research closes a knowledge gap in the field of performative computational architecture. The results of optimization on building performance can be discussed in the three following sections.

### 6.1. Pareto-frontiers solutions

All Pareto fronts (Fig. 12) potentially improved ASE levels in the five climate zones compared to the base model. In Kerman, and Bushehr, direct exposure to sunlight is significantly controlled with 100% total



Fig. 7. SRC for design variables, including WWR and shading characteristics on ASE, sDA, and EUI.

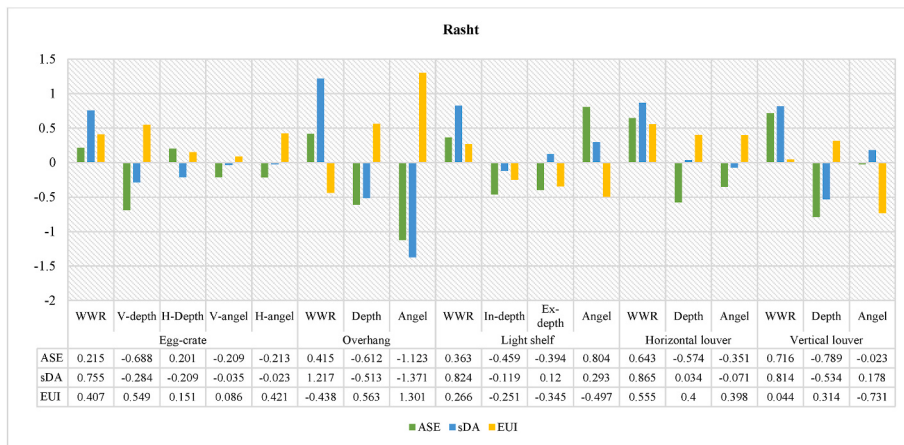


Fig. 7. (continued).

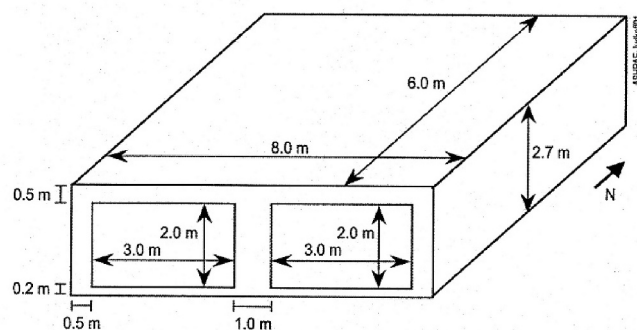


Fig. 8. Case No.600. Ashrae standard 140-2020 [129].

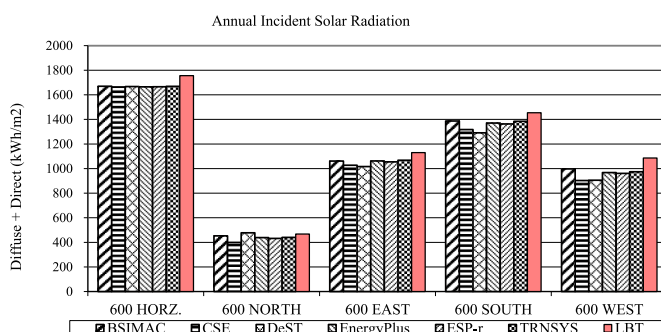


Fig. 9. Result from comparison based on annual incident solar radiation.

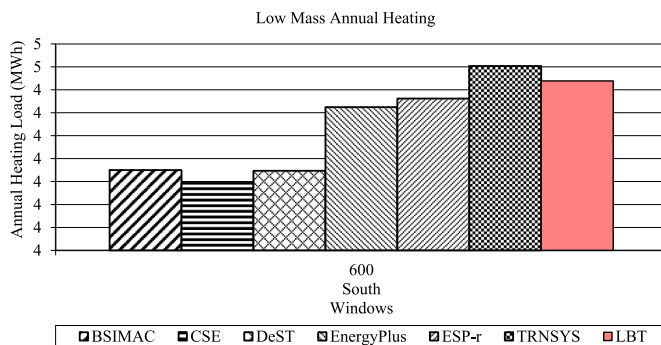


Fig. 10. Result from comparison based on annual heating load.

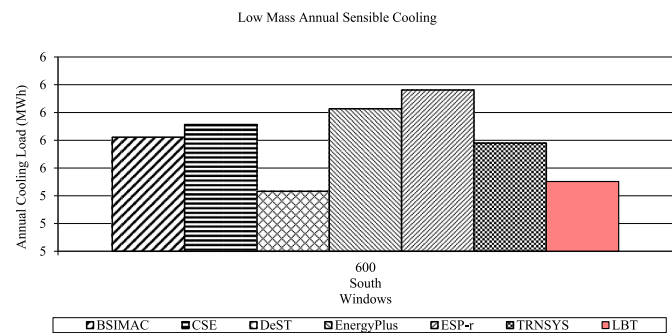


Fig. 11. Result comparison based on annual cooling load.

average ASE improvement, while in Yazd, Mashhad and Rasht, ASE was enhanced by 99.4%, 98.0% and 98.6%, respectively (Fig. 13). Meanwhile, the lowest ASE enhancement is dedicated to the overhang-installed model in Mashhad by 91.4% with 10%WWR, 0.6 m shading depth, and 50° angle. Furthermore, none of the Pareto front solutions could improve sDA, since all the base models provided 100% sDA level across all climate zones. Specifically, the worst daylight performance happened in the overhang-installed model in Rash with 10%WWR, 1 m depth, and -30° angle by 63.69% sDA reduction. The weak performance can be attributed to the mostly cloudy sky of Rasht, which prevents sun radiation from penetrating inside the space.

Results of the energy performance of the Pareto fronts demonstrate that using the studied FESSs could improve building energy efficiency by a total average 28.38%, 23.22%, 21.292%, 18.73%, 14.70%, in Yazd, Bushehr, Kerman, Mashhad, Rasht, respectively and sequentially. It can be inferred that the FESS-integrated facade achieves the greatest energy efficiency in arid climatic zones, such as Yazd and Bushehr, with hot desert and hot semi-arid climates, where solar radiation management is a major problem in reducing building energy demand. However, the least energy-saving is related to Rasht with the Mediterranean climate. Meanwhile, the most improved energy performance is accomplished in V-louver-installed model by 36.81% in Yazd with 20%WWR, 0.2 m depth, and -80° angle, while the minimum energy saving is related to the egg-crater-installed model in Rasht by 12.69% with 10% WWR, 0.5 m, -40° Vertical and 0.3 m, -20° horizontal depth and angle, respectively.

## 6.2. Absolute optimum solutions

The results of the selected optimum genomes on building daylight and energy performances can be discussed as follows:

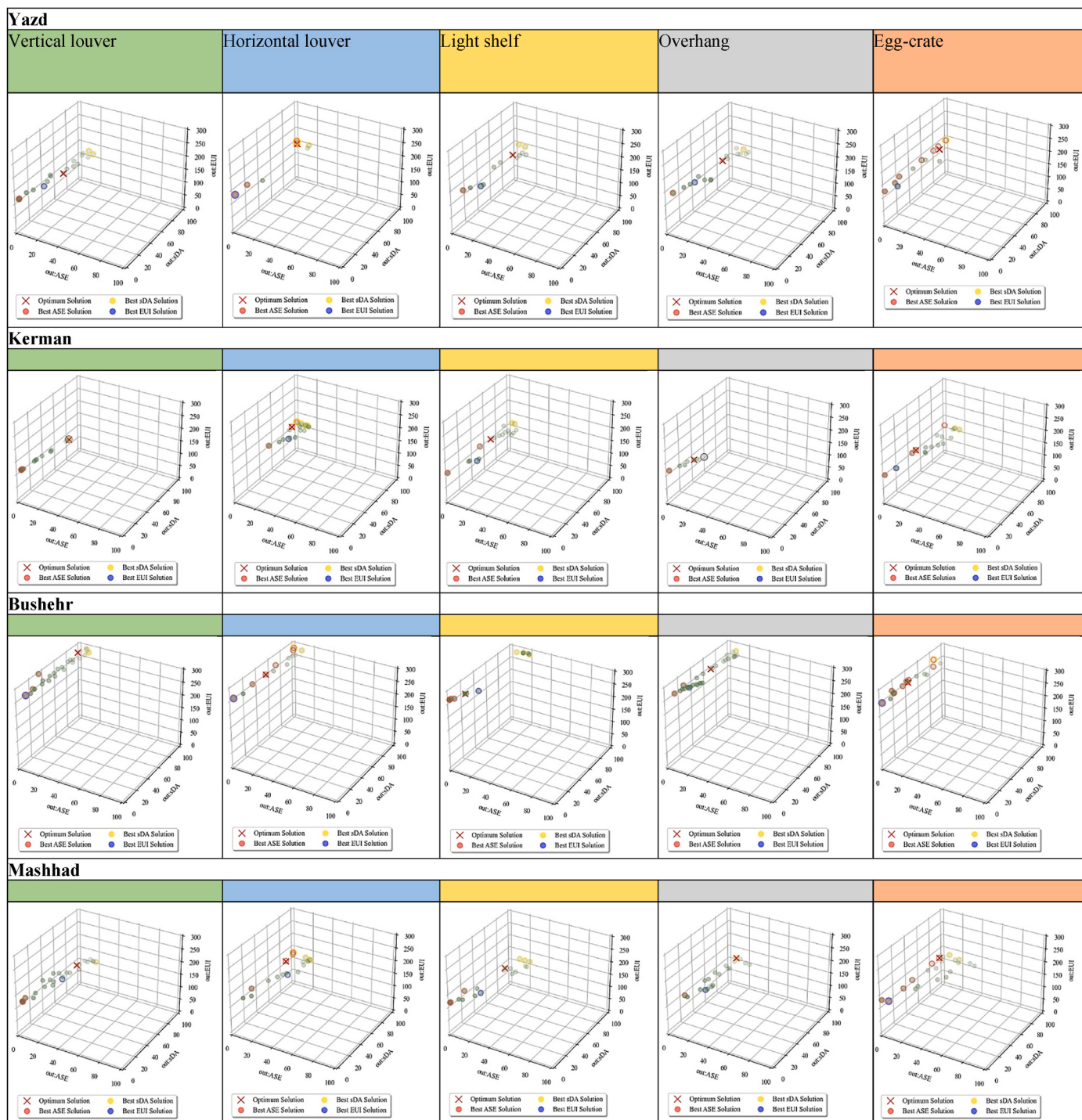


Fig. 12. Pareto optimum genome with illustration of best single-objectives.

- Considering ASE, H-louver overcomes the other systems by contributing to 100% ASE reduction in all climate zones except for Rasht. It can be attributed to the cloudier sky, and the highest altitude ( $37.2713^{\circ}$  N) compared to the other cities with smaller solar radiation angles, which can pass through the H-louver slats. The average contribution of H-louver to ASE in all climate zones is 97.05%, while the lowest average ASE value is dedicated to V-louver by 80.46% (Fig. 14). In general, FESS-integrated façade bestows considerable protection from sun exposure to the space by 95.22%,

90.02%, 89.34%, 89.06%, and 77%, average ASE reduction in Bushehr, Mashhad, Yazd, Kerman, and Yazd, respectively.

- sDA level is reduced in all climate zones excluding the H-louver-installed model in Yazd and Rasht and the overhang-installed model in Mashhad, with no improvement in sDA level compared to the base model. Meanwhile, Mashhad has the lowest average sDA decrease of 11.30%, while Bushehr has the greatest at 46.30%. When comparing each shading system to the base model, egg-crane has the largest sDA average decrease of 40.55%, while H-louver has the lowest at

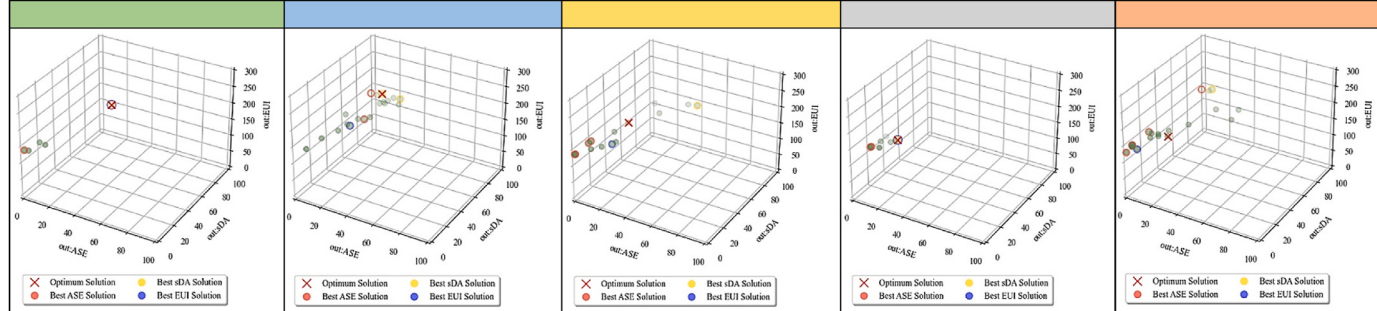
**Rasht**

Fig. 12. (continued).

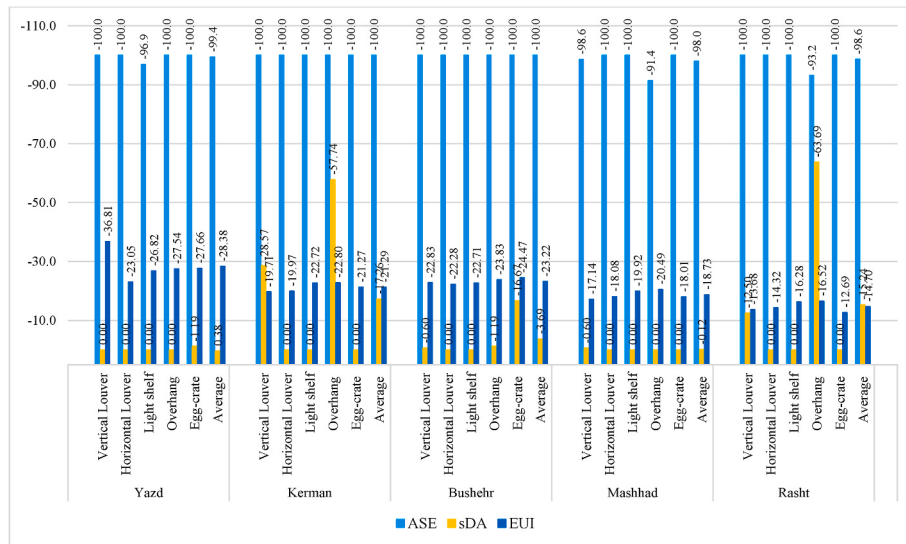


Fig. 13. Fractional impact and total average fractional impact of each FESS on the best single-objective performance (Best ASE, Best sDA, Best EUI).

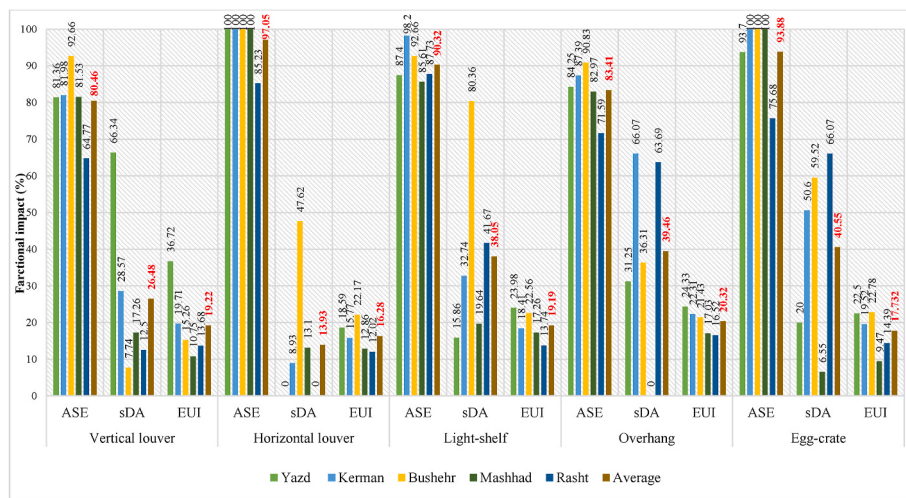


Fig. 14. Average fractional impact of each shading system on performance metrics.

13.93%. In general, H-louver surpasses the other FESSs regarding both sDA and ASE metrics.

- EUI in all Pareto solutions was reduced via MOO process. In Yazd, shading systems provide the highest contribution to EUI at 25.22%, followed by Bushehr, Kerman, Rasht, and Mashhad by 20.84%, 19.14%, 14.06%, and 13.47%, respectively. It can be concluded that

the FESS-integrated facade as a passive design sustainability-oriented strategy can greatly contribute to reducing school energy consumption by controlling sunlight in desert climates, where high solar radiation and the least precipitation compared to other climate zones lead to high cooling energy demand. Besides, the results indicated overhang has the best average EUI improvement by

20.32% in all climate zones, followed by V-louver by 19.22%, light shelf by 19.19%, V-louver by 19.22%, egg-crate by 17.73% and H-louver by 16.28%.

### 6.3. Parameters and performance objectives

Across all climate zones, depth and the angle of overhang have negative effects on sDA and ASE, while they have positive impacts on EUI in Kerman, Mashhad, and Rasht. There is a negative relationship between the depth of overhang and EUI in Yazd. Only in Bushehr, with the highest solar radiation angle, the greater magnitude of angle and depth results in lower EUI. Regarding egg-crate, only vertical angle is positively connected to daylight metrics in all analyzed cities, with the exception of Kerman, where horizontal depth has a positive influence on daylight indices, and Rasht, where horizontal depth only impacts ASE positively. Regarding the light shelf, the greatest dimension of the interior depth results in lower daylight and energy metrics in all cities. However, in Bushehr, interior depth negatively affects sDA the same as the negative influence of exterior depth and angle on EUI. Moreover, in Kerman, with a higher dimension of interior depth, there is lower sDA and EUI values, and higher exterior depth and angle result in lower sDA and EUI levels. The deeper the depth and angle of the H-louver, the lower the daylight metrics occur throughout all climatic types, with the exception of Rasht, where increased depth leads in a higher sDA value. In Yazd, a higher angle provides more energy savings for the H-louver-installed model. By extending the depth of V-louver in any climate type excluding Bushehr, sDA and ASE are decreased; however, EUI is increased.

## 7. Conclusion

This research bridges the knowledge gap in performance-driven architectural design, and passive design strategies by adopting external shading devices in educational buildings across different climate zones of Iran, to define the optimum energy and daylighting performances through the MOO approach. The multi-objective framework can examine sDA, ASE, and EUI metrics in the FESS-integrated facade as a sustainable passive solution for improving energy efficiency and daylight performance. The variable of interest includes WWR and shading characteristics (angle and depth) in a south-orientated classroom façade. Using sample testing case No.600(BESTest), it was concluded that the Honeybee plugin using EnergyPlus and OpenStudio could get ASHRAE Standard 140-2020 validation. The results also indicate a variety of design strategies for FESS-integrated educational buildings to achieve optimum energy and daylight performances. The suggested MOO framework's benefit was proved by its ability to find design combinations that maximize energy efficiency and daylight enhancements for FESS-installed façades. The optimization could improve the EUI and ASE performances of all studied models by applying any shading devices across the entire climate zones. However, considering sDA, some shading systems did not show acceptable performance to achieve the standard levels. These systems include overhang and egg-crate in Kerman and Rasht, as well as light shelf and egg-crate in Bushehr. Meanwhile, egg-crate has the highest energy improvement by 22.78% in Bushehr, and the lowest in Mashhad by 9.47% among absolute optimum solutions in five climate zones. The results of the sensitivity analysis indicated the great influence of WWR on daylight and energy performance indices almost in all climate zones. The ranges of WWR in the absolute optimum solutions are between 20 and 40%, 10–30%, 10–50%, 10–40%, and 10–30% for Yazd, Kerman, Bushehr, Mashhad, and Rasht, respectively. Accordingly, a larger WWR of 50% is permitted for the V-louver-integrated facade in Bushehr, which has the greatest average dry bulb temperature and total sky cover, as well as the lowest latitude, resulting in the largest solar radiation angle among other climatic zones. The lowest WWR of 10% is suggested when the overhang-installed façade is located in Kerman, Mashad, and Rasht and

when the light shelf-installed model is in Bushehr.

The result can be useful for adaptable exterior shading systems due to considering the wide ranges of depths and angles of the shading devices. Future studies might explore integrating FESS with various shading technologies such as PV panels, bio-adaptable shading such as micro-algae photobioreactors, and switchable glazing. They can also examine the role of other variables, such as shading and window materials, different orientations, and building features (height, depth, length, geometry) on other performance metrics like thermal comfort, view quality, cost, CO<sub>2</sub> emission, etc., across other Köppen climate zones. Moreover, the research can be extended by evaluating the role of interior shading systems on building performance and comparing their role with exterior ones.

## CRediT authorship contribution statement

**Maryam Talaei:** Writing – review & editing, Writing – original draft, Visualization, Validation, Supervision, Resources, Project administration, Methodology, Investigation, Formal analysis, Data curation, Conceptualization. **Hamed Sangin:** Visualization, Validation, Software, Resources, Formal analysis, Data curation, Investigation.

## Declaration of competing interest

The authors declare that they have no known competing financial interests or personal relationships that could have appeared to influence the work reported in this paper.

## Data availability

Data will be made available on request.

## Appendix A. Supplementary data

Supplementary data to this article can be found online at <https://doi.org/10.1016/j.buildenv.2024.111424>.

## References

- [1] Cai T. Wang, S. Wang, L. Cozzi, B. Motherway, D. Turk, Towards a zero-emission, efficient, and resilient buildings and construction sector, 2017.
- [2] R. Loonen, J. Rico-Martinez, F. Favoino, M. Brzezicki, C. Menezo, G. La Ferla, et al., Design for façade adaptability: towards a unified and systematic characterization, in: 10th Conf Adv Build Sci, 2015, pp. 1284–1294.
- [3] D. Commission, Energy-efficient buildings :multi-annual roadmap for the contractual PPP under horizon 2020/European commission, directorate-general for research & innovation. National Library, EC - European Commission, 2013.
- [4] V. Hartkopf, A. Aziz, V. Loftness, Facades and enclosures, building for sustainability, in: V. Loftness (Ed.), Sustain. Built Environ. Encycl. Sustain. Sci. Technol. Ser., Springer, New York, 2020, pp. 295–325, [https://doi.org/10.1007/978-1-0716-0684-1\\_873](https://doi.org/10.1007/978-1-0716-0684-1_873).
- [5] Y. Zhou, C.M. Herr, A review of advanced façade system technologies to support net-zero carbon high-rise building design in subtropical China, Sustain. Times 15 (2023), <https://doi.org/10.3390/su15042913>.
- [6] A. Balali, A. Valipour, Identification and selection of building façade's smart materials according to sustainable development goals, Sustain. Mater Technol 26 (2020) e00213, <https://doi.org/10.1016/j.susmat.2020.e00213>.
- [7] S. Habibi, O.P. Valladares, D.M. Peña, Sustainability performance by ten representative intelligent Façade technologies: a systematic review, Sustain. Energy Technol. Assessments 52 (2022), <https://doi.org/10.1016/j.seta.2022.102001>.
- [8] Z. Fan, M. Liu, S. Tang, A multi-objective optimization design method for gymnasium facade shading ratio integrating energy load and daylight comfort, Build. Environ. 207 (2022) 108527, <https://doi.org/10.1016/j.buildenv.2021.108527>.
- [9] A. Vukadinović, J. Radosavljević, A. Đorđević, M. Protić, N. Petrović, Multi-objective optimization of energy performance for a detached residential building with a sunspace using the NSGA-II genetic algorithm, Sol. Energy 224 (2021) 1426–1444, <https://doi.org/10.1016/j.solener.2021.06.082>.
- [10] X. Chen, H. Yang, A multi-stage optimization of passively designed high-rise residential buildings in multiple building operation scenarios, Appl. Energy 206 (2017) 541–557, <https://doi.org/10.1016/j.apenergy.2017.08.204>.
- [11] A. Zhang, R. Bokel, A. van den Dobbelaer, Y. Sun, Q. Huang, Q. Zhang, Optimization of thermal and daylight performance of school buildings based on a

- multi-objective genetic algorithm in the cold climate of China, *Energy Build.* 139 (2017) 371–384. <https://doi.org/10.1016/j.enbuild.2017.01.048>.
- [12] W.K. Alhuwayil, F.A. Almaziad, M. Abdul Mujeebu, Energy performance of passive shading and thermal insulation in multistory hotel building under different outdoor climates and geographic locations, *Case Stud. Therm. Eng.* 45 (2023) 102940. <https://doi.org/10.1016/j.csite.2023.102940>.
- [13] Y. Elaouzy, A. El Fadar, Energy, economic and environmental benefits of integrating passive design strategies into buildings: a review, *Renew. Sustain. Energy Rev.* 167 (2022) 112828. <https://doi.org/10.1016/j.rser.2022.112828>.
- [14] I. Elzeyadi, The impacts of dynamic façade shading typologies on building energy performance and occupant's multi-comfort, *Architect. Sci. Rev.* 60 (2017) 316–324. <https://doi.org/10.1080/00038628.2017.1337558>.
- [15] M. Rabani, H. Bayera Madessa, N. Nord, Achieving zero-energy building performance with thermal and visual comfort enhancement through optimization of fenestration, envelope, shading device, and energy supply system, *Sustain. Energy Technol. Assessments* 44 (2021) 101020. <https://doi.org/10.1016/j.seta.2021.101020>.
- [16] A. Monge-Barrio, A. Sánchez-Ostiz Gutiérrez, Passive Energy Strategies for Mediterranean Residential Buildings: Facing the Challenges of Climate Change and Vulnerable Populations, Springer.
- [17] S. Mousavi, M. Gijón-Rivera, C.I. Rivera-Solorio, C. Godoy Rangel, Energy, comfort, and environmental assessment of passive techniques integrated into low-energy residential buildings in semi-arid climate, *Energy Build.* 263 (2022) 112053. <https://doi.org/10.1016/j.enbuild.2022.112053>.
- [18] Q. Xue, Z. Wang, Q. Chen, Multi-objective optimization of building design for life cycle cost and CO<sub>2</sub> emissions: A case study of a low-energy residential building in a severe cold climate, *Build. Simul.* 15 (2022) 83–98. <https://doi.org/10.1007/s12273-021-0796-5>.
- [19] R.P. Khidmat, H. Fukuda, Kustiani, B. Paramita, M. Qingsong, A. Hariyadi, Investigation into the daylight performance of expanded-metal shading through parametric design and multi-objective optimisation in Japan, *J. Build. Eng.* 51 (2022) 104241. <https://doi.org/10.1016/j.jobe.2022.104241>.
- [20] H. Sghouri, A. Mezrab, M. Karkri, H. Naji, Shading devices optimization to enhance thermal comfort and energy performance of a residential building in Morocco, *J. Build. Eng.* 18 (2018) 292–302. <https://doi.org/10.1016/J.JOBE.2018.03.018>.
- [21] K. Lakhdari, L. Sriti, B. Painter, Parametric optimization of daylight, thermal and energy performance of middle school classrooms, case of hot and dry regions, *Build. Environ.* 204 (2021) 108173. <https://doi.org/10.1016/j.buildenv.2021.108173>.
- [22] A. Kirimtak, O. Krejcar, B. Ekici, M. Fatih Tagetiren, Multi-objective energy and daylight optimization of amorphous shading devices in buildings, *Sol. Energy.* 185 (2019) 100–111. <https://doi.org/10.1016/j.solener.2019.04.048>.
- [23] G. Chiesa, A. Acquaviva, M. Grossi, L. Bottaccioli, M. Floridia, E. Pristeri, E. M. Sanna, Parametric optimization of window-to-wall ratio for passive buildings adopting a scripting methodology to dynamic-energy simulation, *Sustain.* 11 (2019). <https://doi.org/10.3390/su1113078>.
- [24] M. Sedaghatnia, M. Faizi, M. Khakzand, H. Sanaieian, Energy and daylight optimization of shading devices, window size, and orientation for educational spaces in Tehran, Iran, *J. Archit. Eng.* 27 (2021) 04021011. [https://doi.org/10.1061/\(ASCE\)AE.1943-5568.0000466](https://doi.org/10.1061/(ASCE)AE.1943-5568.0000466).
- [25] Y. Fang, S. Cho, Design optimization of building geometry and fenestration for daylighting and energy performance, *Sol. Energy.* 191 (2019) 7–18. <https://doi.org/10.1016/j.solener.2019.08.039>.
- [26] B.J. Alkhataeb, Y. Kurdi, S. Asadi, Multi-Objective Optimization of Classrooms' Daylight Performance and Energy Use in U.S. Climate Zones, *Energy Build.* (Under Rev.) (2023) 113468. <https://doi.org/10.1016/j.enbuild.2023.113468>.
- [27] A. Khani, M. Khakzand, M. Faizi, Multi-objective optimization for energy consumption, visual and thermal comfort performance of educational building (case study: Qeshm Island, Iran), *Sustain. Energy Technol. Assessments.* 54 (2022) 102872. <https://doi.org/10.1016/j.seta.2022.102872>.
- [28] H. Wu, T. Zhang, Multi-objective optimization of energy, visual, and thermal performance for building envelopes in China's hot summer and cold winter climate zone, *J. Build. Eng.* 59 (2022) 105034. <https://doi.org/10.1016/j.jobe.2022.105034>.
- [29] M. Baghoolizadeh, M. Rostamzadeh-Renani, R. Rostamzadeh-Renani, D. Toghraie, Multi-objective optimization of Venetian blinds in office buildings to reduce electricity consumption and improve visual and thermal comfort by NSGA-II, *Energy Build.* 278 (2023) 112639. <https://doi.org/10.1016/j.enbuild.2022.112639>.
- [30] J. Zhao, Y. Du, Multi-objective optimization design for windows and shading configuration considering energy consumption and thermal comfort: A case study for office building in different climatic regions of China, *Sol. Energy.* 206 (2020) 997–1017. <https://doi.org/10.1016/j.solener.2020.05.090>.
- [31] N. Nasrollahzadeh, Comprehensive building envelope optimization: Improving energy, daylight, and thermal comfort performance of the dwelling unit, *J. Build. Eng.* 44 (2021) 103418. <https://doi.org/10.1016/j.jobe.2021.103418>.
- [32] M. Khoroshiltseva, D. Slanzi, I. Poli, A Pareto-based multi-objective optimization algorithm to design energy-efficient shading devices, *Appl. Energy.* 184 (2016) 1400–1410. <https://doi.org/10.1016/j.apenergy.2016.05.015>.
- [33] H. Kim, M.J. Clayton, A multi-objective optimization approach for climate-adaptive building envelope design using parametric behavior maps, *Build. Environ.* 185 (2020) 107292. <https://doi.org/10.1016/j.buildenv.2020.107292>.
- [34] A. Ciardiello, F. Rosso, J. Dell'Olmo, V. Ciancio, M. Ferrero, F. Salata, Multi-objective approach to the optimization of shape and envelope in building energy design, *Appl. Energy.* 280 (2020) 115984. <https://doi.org/10.1016/j.apenergy.2020.115984>.
- [35] X. Chen, H. Yang, W. Zhang, Simulation-based approach to optimize passively designed buildings: A case study on a typical architectural form in hot and humid climates, *Renew. Sustain. Energy Rev.* 82 (2018) 1712–1725. <https://doi.org/10.1016/j.rser.2017.06.018>.
- [36] A. Ebrahimi-Moghadam, P. Ildarabadi, K. Aliakbari, F. Fadaee, Sensitivity analysis and multi-objective optimization of energy consumption and thermal comfort by using interior light shelves in residential buildings, *Renew. Energy.* 159 (2020) 736–755. <https://doi.org/10.1016/j.renene.2020.05.127>.
- [37] R.A. Mangkuto, D.K. Dewi, A.A. Herwandani, M.D. Koerniawan, Faridah, Design optimisation of internal shading device in multiple scenarios: Case study in Bandung, Indonesia, *J. Build. Eng.* 24 (2019) 100745. <https://doi.org/10.1016/j.jobe.2019.100745>.
- [38] Y. Xu, G. Zhang, C. Yan, G. Wang, Y. Jiang, K. Zhao, A two-stage multi-objective optimization method for envelope and energy generation systems of primary and secondary school teaching buildings in China, *Build. Environ.* 204 (2021) 108142. <https://doi.org/10.1016/j.buildenv.2021.108142>.
- [39] N. Castilla, C. Llinares, F. Biseagna, V. Blanca-Giménez, Emotional evaluation of lighting in university classrooms: A preliminary study, *Front. Archit. Res.* 7 (2018) 600–609. <https://doi.org/10.1016/j.fjor.2018.07.002>.
- [40] S. Subhashini, K. Thirumaran, A passive design solution to enhance thermal comfort in an educational building in the warm humid climatic zone of Madurai, *J. Build. Eng.* 18 (2018) 395–407. <https://doi.org/10.1016/j.jobe.2018.04.014>.
- [41] J.H. Park, B.Y. Yun, S.J. Chang, S. Wi, J. Jeon, S. Kim, Impact of a passive retrofit shading system on educational building to improve thermal comfort and energy consumption, *Energy Build.* 216 (2020). <https://doi.org/10.1016/j.enbuild.2020.109930>.
- [42] B.J. Wachenfeldt, M. Mysen, P.G. Schild, Air flow rates and energy saving potential in schools with demand-controlled displacement ventilation, *Energy Build.* 39 (2007) 1073–1079. <https://doi.org/10.1016/J.ENBUILD.2006.10.018>.
- [43] D.A. Coley, R. Greeves, B.K. Saxby, The Effect of Low Ventilation Rates on the Cognitive Function of a Primary School Class, *International Journal of Ventilation* 6 (2016) 107–112. <https://doi.org/10.1080/14733315.2007.11683770>.
- [44] B. Lala, A. Hagishima, A Review of Thermal Comfort in Primary Schools and Future Challenges in Machine Learning Based Prediction for Children, *Buildings* 12 (2022). <https://doi.org/10.3390/buildings12112007>.
- [45] S. Mohammad, A. Shea, Performance Evaluation of Modern Building Thermal Envelope Designs in the Semi-Arid Continental Climate of Tehran, *Build.* 2013, Vol. 3, Pages 674–688. 3 (2013) 674–688. <https://doi.org/10.3390/BUILDINGS3040674>.
- [46] E. Rodrigues, N.A. Fereidan, M.S. Fernandes, A.R. Gaspar, Climate change and ideal thermal transmittance of residential buildings in Iran, *J. Build. Eng.* 74 (2023) 106919. <https://doi.org/10.1016/J.JOBE.2023.106919>.
- [47] N. Ziae, R. Vakilinezhad, Multi-objective optimization of daylight performance and thermal comfort in classrooms with light-shelves: Case studies in Tehran and Sari, Iran, *Energy Build.* 254 (2022) 111590. <https://doi.org/10.1016/j.enbuild.2021.111590>.
- [48] M. Rakhsani Mehr, D. Varnaseri, S. MEmarian, F. Zare, A.M. Shabazi, M. Khalili, E. Makhdoomi, S. Hosseiniinia, M. Khebreh, R. Fayaz, S.M. Mofidi Shemiran, A.S. Mahmoudi, M. Tahbaz, K. Fattahi, H. Jahanbakhsh, A. Azemati, A. Salehi, M. Heiranipour, M. Abbasi, seyyed A. Tayyari, Integrated design process of green school, *Sherkat Tarrahan katibeh Iranian, Tehran*, 2020.
- [49] A. Kirimtak, B.K. Koyunbaba, I. Chatzikonstantinou, S. Sarıyıldız, Review of simulation modeling for shading devices in buildings, *Renew. Sustain. Energy Rev.* 53 (2016) 23–49. <https://doi.org/10.1016/j.rser.2015.08.020>.
- [50] J. Cho, C. Yoo, Y. Kim, Viability of exterior shading devices for high-rise residential buildings: Case study for cooling energy saving and economic feasibility analysis, *Energy Build.* 82 (2014) 771–785. <https://doi.org/10.1016/j.enbuild.2014.07.092>.
- [51] J. Al Dakheel, K.T. Aoul, Building applications, opportunities and challenges of active shading systems: A state-of-the-art review, *Energies* 10 (2017). <https://doi.org/10.3390/en10101672>.
- [52] E.S. Lee, S.E. Selkowitz, G.D. Hughes, D. a. Thurm, Market transformation opportunities for emerging dynamic façade and dimmable lighting control systems, in: *ACEEE Summer Study Energy Effic. Build.* (2004) 0–10.
- [53] M. Talaei, M. Mahdavinejad, R. Azari, H.M. Haghghi, A. Atashdast, Thermal and energy performance of a user-responsive microalgae bioreactive façade for climate adaptability, *Sustain. Energy Technol. Assessments.* 52 (2022) 101894. <https://doi.org/10.1016/J.SETA.2021.101894>.
- [54] A. Cots, S. Dicorato, L. Giovannini, F. Favoino, M. Manca, Energy efficient smart plasmochromic Windows: properties, manufacturing and integration in insulating Glazing, *Nano Energy* 84 (2021) 105894. <https://doi.org/10.1016/J.NANOEN.2021.105894>.
- [55] F. Favoino, L. Giovannini, R. Loonen, Smart glazing in Intelligent Buildings: what can we simulate?, in: *GPD 2017 - Glas. Perform. Days 2017*, Tampere, Finland, 2017: pp. 8–15.
- [56] M. Casini, Energy-generating glazing, *Smart Build.* (2016) 327–353. <https://doi.org/10.1016/b978-0-08-100635-1.00010-1>.
- [57] P. Jayathissa, M. Luzzatto, J. Schmidli, J. Hofer, Z. Nagy, A. Schlueter, Optimising building net energy demand with dynamic BIPV shading, *Appl. Energy*. 202 (2017) 726–735. <https://doi.org/10.1016/j.apenergy.2017.05.083>.
- [58] A. Tabadkani, A. Roetzel, H.X. Li, A. Tsangrassoulis, Design approaches and typologies of adaptive facades: A review, *Autom. Constr.* 121 (2021) 103450. <https://doi.org/10.1016/j.autcon.2020.103450>.

- [59] F. De Luca, H. Voll, M. Thalfeldt, Comparison of static and dynamic shading systems for office building energy consumption and cooling load assessment, *Manag. Environ. Qual. An Int. J.* 29 (2018) 978–998. <https://doi.org/10.1108/MEQ-01-2018-0008>.
- [60] S.M. Al-Masrani, K.M. Al-Obaidi, N.A. Zalin, M.I. Aida Isma, Design optimisation of solar shading systems for tropical office buildings: Challenges and future trends, *Sol. Energy.* 170 (2018) 849–872. <https://doi.org/10.1016/j.solener.2018.04.047>.
- [61] R.A. Mangkuto, M.D. Koerniawan, S.R. Apriliyanthi, I.H. Lubis, Atthaillah, J.L.M. Hensen, B. Paramita, Design Optimisation of Fixed and Adaptive Shading Devices on Four Façade Orientations of a High-Rise Office Building in the Tropics, *Buildings.* 12 (2022). <https://doi.org/10.3390/buildings12010025>.
- [62] S. Attia, S. Bilir, T. Safy, C. Struck, R. Loonen, F. Goia, Current trends and future challenges in the performance assessment of adaptive façade systems, *Energy Build.* 179 (2018) 165–182. <https://doi.org/10.1016/j.enbuild.2018.09.017>.
- [63] A. Tsangaroulis, Shading and Daylight Systems, in: S.-N. Boemi, O. Irulegi, M. Santamouris (Eds.), *Energy Perform. Build. Energy Effic. Built Environ.*, Springer, 2016, pp. 437–466. [https://doi.org/10.1007/978-3-319-20831-2\\_21](https://doi.org/10.1007/978-3-319-20831-2_21).
- [64] L. Bellia, C. Marino, F. Minichiello, A. Pedace, An overview on solar shading systems for buildings, *Energy Procedia* 62 (2014) 309–317. <https://doi.org/10.1016/j.egypro.2014.12.392>.
- [65] A. Atzeri, F. Cappelletti, A. Gasparella, Internal versus external shading devices performance in office buildings, *Energy Procedia* 45 (2014) 463–472. <https://doi.org/10.1016/j.egypro.2014.01.050>.
- [66] F. De Luca, H. Voll, M. Thalfeldt, Horizontal or vertical? Windows' layout selection for shading devices optimization, *Manag. Environ. Qual. An Int. J.* 27 (2016) 623–633. <https://doi.org/10.1108/MEQ-05-2015-0102>.
- [67] S.M. Elouadjjeri, A. Boussoalim, H. Ait Haddou, Evaluating the Effect of External Horizontal Fixed Shading Devices' Geometry on Internal Air Temperature, Daylighting and Energy Demand in Hot Dry Climate. Case Study of Ghardaïa, Algeria, *Buildings* 11 (2021). <https://doi.org/10.3390/buildings11080348>.
- [68] M. Krarti, Evaluation of energy performance of dynamic overhang systems for US residential buildings, *Energy Build.* 234 (2021) 110699. <https://doi.org/10.1016/j.enbuild.2020.110699>.
- [69] D. Ouahrami, A. Al Touma, Selection of slat separation-to-width ratio of brise-soleil shading considering energy savings, CO<sub>2</sub> emissions and visual comfort – a case study in Qatar, *Energy Build.* 165 (2018) 440–450. <https://doi.org/10.1016/j.enbuild.2017.12.053>.
- [70] G. Kim, H.S. Lim, T.S. Lim, L. Schaefer, J.T. Kim, Comparative advantage of an exterior shading device in thermal performance for residential buildings, *Energy Build.* 46 (2012) 105–111. <https://doi.org/10.1016/j.enbuild.2011.10.040>.
- [71] J. Settino, C. Carpino, S. Perrella, N. Arcuri, Multi-objective analysis of a fixed solar shading system in different climatic areas, *Energies* 13 (2020). <https://doi.org/10.3390/en13123249>.
- [72] B. Ekici, C. Cubukcuoglu, M. Turrin, I.S. Sarıyıldız, Performative computational architecture using swarm and evolutionary optimisation: A review, *Build. Environ.* 147 (2019) 356–371. <https://doi.org/10.1016/j.buildenv.2018.10.023>.
- [73] A. Tsangaroulis, in: S.-N. Boemi, O. Irulegi, M. Santamouris (Eds.), *Build. Energy Effic. Built Environ. Temp. Clim.* (2016) 437–466. [https://doi.org/10.1007/978-3-319-20831-2\\_21](https://doi.org/10.1007/978-3-319-20831-2_21).
- [74] Y. Geng, B. Lin, Y. Zhu, Comparative study on indoor environmental quality of green office buildings with different levels of energy use intensity, *Build. Environ.* 168 (2020) 106482. <https://doi.org/10.1016/j.buildenv.2019.106482>.
- [75] P. Shen, Z. Wang, How neighborhood form influences building energy use in winter design condition : Case study of Chicago using CFD coupled simulation, *J. Clean. Prod.* 261 (2020) 121094. <https://doi.org/10.1016/j.jclepro.2020.121094>.
- [76] P. Wang, Y. Yang, C. Ji, L. Huang, Influence of built environment on building energy consumption: a case study in Nanjing, China, *Environ. Dev. Sustain.* (2023). <https://doi.org/10.1007/s10668-023-02930-w>.
- [77] M.T. L. Heschong, V.D. Wymelenberg, Keven, M. Andersen, N. Digert, L. Fernandes, A. Keller, J. Loveland, H. McKay, R. Mistrick, B. Mosher, C. Reinhart, Z. Rogers, Approved Method: IES Spatial Daylight Autonomy (sDA) and Annual Sunlight Exposure (ASE), (2012).
- [78] T. Kazanasmaz, L.O. Grobe, C. Bauer, M. Krehel, S. Wittkopf, Three approaches to optimize optical properties and size of a South-facing window for spatial Daylight Autonomy, *Build. Environ.* 102 (2016) 243–256. <https://doi.org/10.1016/j.buildenv.2016.03.018>.
- [79] P. Pilechiha, M. Mahdavinejad, F. Pour Rahimian, P. Carnemolla, S. Seyedzadeh, Multi-objective optimisation framework for designing office windows: quality of view, daylight and energy efficiency, *Appl. Energy.* 261 (2020) 114356. <https://doi.org/10.1016/j.apenergy.2019.114356>.
- [80] SLL Code for Lighting, London, 2022.
- [81] S.M. Haakonsen, S.H. Dyyik, M. Luczkowski, A. Rønquist, A Grasshopper Plugin for Finite Element Analysis with Solid Elements and Its Application on Gridshell Nodes, *Appl. Sci.* 12 (2022). <https://doi.org/10.3390/app12126037>.
- [82] M.S. Roudsari, M. Pak, LADYBUG: A parametric environmental plugin FORFOR grasshopper to help designers create an environmentally-conscious design, in: BS2013-13th Int. Conf. Build. Perform. Simul. Assoc., Chambery, France, 2013: pp. 3128–3135.
- [83] Y. Zhai, Y. Wang, Y. Huang, X. Meng, A multi-objective optimization methodology for window design considering energy consumption, thermal environment and visual performance, *Renew. Energy.* 134 (2019) 1190–1199. <https://doi.org/10.1016/j.renene.2018.09.024>.
- [84] I.G. Dino, G. Üçoluk, Multiobjective Design Optimization of Building Space Layout, Energy, and Daylighting Performance, *J. Comput. Civ. Eng.* 31 (2017) 04017025. [https://doi.org/10.1061/\(asce\)cp.1943-5487.0000669](https://doi.org/10.1061/(asce)cp.1943-5487.0000669).
- [85] D.E. Knebel, T.P. McDowell, S.J. Emmerich, D.M. Brundage, J.M. Ferguson, M.W. Gallagher, W.T. Grondzik, S.S. Hanson, R.L. Hedrick, J. Humble, Standard method of test for the evaluation of building energy analysis computer programs, *ASHRAE Stand.* (2017) (2004) 404–636.
- [86] M.T. Aguilar-Carrasco, J. Díaz-Borrego, I. Acosta, M.Á. Campano, S. Domínguez-Amarillo, Validation of lighting parametric workflow tools of Ladybug and Solemma using CIE test cases, *J. Build. Eng.* 64 (2023). <https://doi.org/10.1016/j.jobe.2022.105608>.
- [87] C.F. Reinhart, O. Walkenhorst, Validation of dynamic RADIANCE-based daylight simulations for a test office with external blinds, *Energy Build.* 33 (2001) 683–697. [https://doi.org/10.1016/S0378-7788\(01\)00058-5](https://doi.org/10.1016/S0378-7788(01)00058-5).
- [88] I. Acosta, C. Muñoz, P. Esquivias, D. Moreno, J. Navarro, Analysis of the accuracy of the sky component calculation in daylighting simulation programs, *Sol. Energy.* 119 (2015) 54–67. <https://doi.org/10.1016/j.solener.2015.06.022>.
- [89] Maamarim F, ed., Test cases to assess the accuracy of lighting computer programs, commission international d'Eclairage (CIE) Technical Committee TC3.33., 2006.
- [90] M.H. Ganji, The climate of Iran, *Bull. La Socie'te' Ge'ographie d' Egypte.* 28 (1954) 195–298.
- [91] M. Dehsara, An agro-climatological map of Iran, *Arch. Für Meteorol. Geophys. Und Bioklimatologie Ser. B.* 21 (1973) 393–402. <https://doi.org/10.1007/BF02253315/METRICS>.
- [92] M. Djamali, H. Akhani, R. Khoshravesh, V. Andrieu-Ponel, P. Ponel, S. Brewer, Application of the Global Bioclimatic Classification to Iran: implications for understanding the modern vegetation and biogeography, *Ecol. Mediterr.* 37 (2011) 91–114. <https://doi.org/10.3406/ecmed.2011.1350>.
- [93] Shafi Javadi, Distribution climatiques en Iran, *Monographie de La Me'te'o, Nationale, Paris,* p. 1966.
- [94] A. Khalili, S. Hajam, P. Irannejad, Integrated water plan of Iran, in: Meteorological studies, climatical classification map 1964–1984, Jamab Consulting Engineering, Co., The Ministry of Energy, Tehran, 1992.
- [95] H. Sabeti, Bioclimatic Studies of Iran (in Persian), University of Tehran Press, 1969.
- [96] M. Kasmaei, Climate classification of Iran-Education buildings, *The Organization for Development, Renovation and Equipping Schools (DRES)*, 1990.
- [97] T. Raziei, Climate of Iran according to Köppen-Geiger, Feddeema, and UNEP climate classifications, *Theor. Appl. Climatol.* 148 (2022) 1395–1416. <https://doi.org/10.1007/s00704-022-03992-y>.
- [98] D. Chen, H.W. Chen, Using the Köppen classification to quantify climate variation and change: An example for 1901–2010, *Environ. Dev.* 6 (2013) 69–79. <https://doi.org/10.1016/j.envdev.2013.03.007>.
- [99] B. Omarov, S.A. Memon, J. Kim, A novel approach to develop climate classification based on degree days and building energy performance, *Energy* 267 (2023) 126514. <https://doi.org/10.1016/j.energy.2022.126514>.
- [100] Climate.onebuilding.org, (2020). [http://climate.onebuilding.org/WMO\\_Regional\\_2\\_Asia/IRN\\_Iran/index.html](http://climate.onebuilding.org/WMO_Regional_2_Asia/IRN_Iran/index.html) (accessed June 8, 2020).
- [101] R.M. Ahmad, R.M. Reffat, A comparative study of various daylighting systems in office buildings for improving energy efficiency in Egypt, *J. Build. Eng.* 18 (2018) 360–376. <https://doi.org/10.1016/j.jobe.2018.04.002>.
- [102] Y. Grobman, G. Austern, Y. Hatiel, I. Capeluto, Evaluating the Influence of Varied External Shading Elements on Internal Daylight Illuminances, *Buildings* 10 (2020) 22. <https://doi.org/10.3390/buildings10020022>.
- [103] R.P. Khidmat, H. Fukuda, B. Paramita, M.D. Koerniawan, Kustiani, The optimization of louvers shading devices and room orientation under three different sky conditions, *J. Daylighting.* 9 (2022) 137–149. <https://doi.org/10.15627/jd.2022.11>.
- [104] J. Du, X. Zhang, D. King, An investigation into the risk of night light pollution in a glazed office building: The effect of shading solutions, *Build. Environ.* 145 (2018) 243–259. <https://doi.org/10.1016/j.buildenv.2018.09.029>.
- [105] P.M. Esquivias, C.M. Munoz, I. Acosta, D. Moreno, J. Navarro, Climate-based daylight analysis of fixed shading devices in an open-plan office, *Light. Res. Technol.* 48 (2016) 205–220. <https://doi.org/10.1177/1477153514563638>.
- [106] Y. Zou, S. Lou, D. Xia, I.Y.F. Lun, J. Yin, Multi-objective building design optimization considering the effects of long-term climate change, *J. Build. Eng.* 44 (2021) 102904. <https://doi.org/10.1016/j.jobe.2021.102904>.
- [107] Y. Zou, Q. Zhan, K. Xiang, A comprehensive method for optimizing the design of a regular architectural space to improve building performance, *Energy Reports* 7 (2021) 981–996. <https://doi.org/10.1016/j.egyr.2021.01.097>.
- [108] L. Huang, C. Fan, Z. (John) Zhai, A graphical multi-objective performance evaluation method with architect-friendly mode, *Front. Archit. Res.* 10 (2021) 420–431. <https://doi.org/10.1016/j.foar.2020.12.004>.
- [109] N. Queiroz, F.S. Westphal, F.O. Ruttay Pereira, A performance-based design validation study on EnergyPlus for daylighting analysis, *Build. Environ.* 183 (2020). <https://doi.org/10.1016/j.buildenv.2020.10708>.
- [110] G.A. Warrier, B. Raphael, Performance evaluation of light shelves, *Energy Build.* 140 (2017) 19–27. <https://doi.org/10.1016/j.buildenv.2017.01.068>.
- [111] A. Zhang, Y. Li, Thermal conductivity of aluminum alloys—A Review, *Materials (Basel)* 16 (2023). <https://doi.org/10.3390/ma16082972>.
- [112] L. Bellia, F. De Falco, F. Minichiello, Effects of solar shading devices on energy requirements of standalone office buildings for Italian climates, *Appl. Therm. Eng.* 54 (2013) 190–201. <https://doi.org/10.1016/j.applthermeng.2013.01.039>.
- [113] R.K. Arora, *Optimization: Algorithms and Applications*, Taylor & Francis Group, LLC, 2015.

- [114] M. Caramia, P. Caramia. Multi-objective management in Freight Logistics, Springer, Cham, 2020. <https://doi.org/10.1007/978-3-030-50812-8>.
- [115] D.J. Livingstone. Artificial Neural Networks, Humana, Totowa, NJ, 2009. <https://doi.org/10.1007/978-1-60327-101-1>.
- [116] G. Kumar, N. Parimala. A sensitivity analysis on weight sum method MCDM approach for product recommendation, Springer International Publishing, 2019. [https://doi.org/10.1007/978-3-030-05366-6\\_15](https://doi.org/10.1007/978-3-030-05366-6_15).
- [117] A. Toutou, A Parametric Approach for Achieving Optimum Residential Building A Parametric Approach for Achieving Optimum Residential Building Performance in Hot Arid Zone, Alexandria University.
- [118] X.-S. Yang, Multi-Objective Optimization, in: Nature-Inspired Optim. Algorithms, Elsevier, 2014, pp. 197–211. <https://doi.org/10.1016/B978-0-12-416743-8.00014-2>.
- [119] P. Bakmohammadi, E. Noorzai, Optimization of the design of the primary school classrooms in terms of energy and daylight performance considering occupants' thermal and visual comfort, Energy Reports 6 (2020) 1590–1607. <https://doi.org/10.1016/j.egyr.2020.06.008>.
- [120] M. Talaei, M. Mahdavinejad, R. Azari, A. Prieto, H. Sangin, Multi-objective optimization of building-integrated microalgae photobioreactors for energy and daylighting performance, J. Build. Eng. 42 (2021) 102832. <https://doi.org/10.1016/j.jobe.2021.102832>.
- [121] Y. Shahbazi, M. Heydari, F. Haghparast, An early-stage design optimization for office buildings' façade providing high-energy performance and daylight, Indoor Built Environ 28 (2019) 1350–1367. <https://doi.org/10.1177/1420326X19840761>.
- [122] E. Touloupaki, T. Theodosiou, Optimization of Building form to Minimize Energy Consumption through Parametric Modelling, Procedia Environ. Sci. 38 (2017) 509–514. <https://doi.org/10.1016/j.proenv.2017.03.114>.
- [123] J. Bader, E. Zitzler, HypE: An Algorithm for Fast Hypervolume-Based Many-Objective Optimization, Evol. Comput. 19 (2011) 45–76.
- [124] A.P. Guerreiro, C.M. Fonseca, L. Paquete, The Hypervolume Indicator: Computational Problems and Algorithms, ACM Comput. Surv. 54 (2021). <https://doi.org/10.1145/3453474>.
- [125] N. Brown, J. Ochsendorf, C. Mueller, J. de Oliveira, Early-stage integration of architectural and structural performance in a parametric multi-objective design tool, Struct. Archit. - Proc. 3rd Int. Conf. Struct. Archit. ICSA (2016). (2016) 1103–1111. <https://doi.org/10.1201/b20891-152>.
- [126] N.C. Brown, V. Jusiega, C.T. Mueller, Implementing data-driven parametric building design with a flexible toolbox, Autom. Constr. 118 (2020) 103252. <https://doi.org/10.1016/j.autcon.2020.103252>.
- [127] Z. Pang, Z. O'Neill, Y. Li, F. Niu, The role of sensitivity analysis in the building performance analysis: A critical review, Energy Build 209 (2020) 109659. <https://doi.org/10.1016/j.enbuild.2019.109659>.
- [128] P. Hoseinzadeh, M. Khalaji, S. Heidari, M. Khalatbari, R. Saidur, K. Haghhighat, H. Sangin, Energy performance of building integrated photovoltaic high-rise building : Case study, Energy Build 235 (2021) 110707. <https://doi.org/10.1016/j.enbuild.2020.110707>.
- [129] J. Neymark, T.P. McDowell, M.J. Witte, N.J. Kruis, A. Roth, P. Strachan, M. Tosh, C.S. Barnaby, R.B. Burkhead, S.S. Hanson. ANSI/ASHRAE Standard 140-2020-Method of Test for Evaluating Building Performance Simulation Software, ASHRAE, 2021.
- [130] Y. Wang, W. Yang, Q. Wang, Multi-objective parametric optimization of the composite external shading for the classroom based on lighting, energy consumption, and visual comfort, Energy Build 275 (2022) 112441. <https://doi.org/10.1016/j.enbuild.2022.112441>.